

Turbo and Raptor Coded SIC Receiver Performance
for the Coexistence of LTE and Wi-Fi

Yunfeng Gao

A Thesis

in

The Department

of

Electrical and Computer Engineering

Presented in Partial Fulfillment of the Requirements

for the Degree of Master of Applied Science at

Concordia University

Montreal, Quebec, Canada

March 2015

© Yunfeng Gao, 2015

**CONCORDIA UNIVERSITY
SCHOOL OF GRADUATE STUDIES**

This is to certify that the thesis prepared

By: Yunfeng Gao

Entitled: "Tubro and Raptor Coded SIC Receiver Performance
for the Coexistence of LTE and Wi-Fi"

and submitted in partial fulfillment of the requirements for the degree of

Master of Applied Science

complies with the regulations of the University and meets the accepted standards with respect to originality and quality.

Signed by the final examining committee:

_____ Chair
Dr. M. Z. Kabir

_____ External Examiner
Dr. A. S. Ramamurthy (BCEE)

_____ Examiner
Dr. M. Mehmet-Ali

_____ Thesis Supervisor
Dr. M.R. Soleymani

Approved by _____
Dr. W. E. Lynch, Chair
Department of Electrical and Computer Engineering

March 2015

Dr. Amir Asif, Dean
Faculty of Engineering and Computer Science

Abstract

Turbo and Raptor Coded SIC Receiver Performance

for the Coexistence of LTE and Wi-Fi

Yunfeng Gao

In this thesis, a coexistence of LTE and Wi-Fi is proposed. We assume that both LTE and Wi-Fi transmit in the same band simultaneously, the Wi-Fi signal, which is assumed to be the stronger signal, can be decoded first. We can achieve a good performance of LTE transmission by using a Successive Interference Cancellation (SIC) scheme. The LTE signal, which is the weaker signal, can be decoded successfully as though there is no Wi-Fi interference. We implement a Raptor code for Wi-Fi and a Turbo code for LTE. By adjusting the code rate, the Raptor codes are adaptive to different channel conditions especially with interference. Meanwhile, the Turbo codes are standardized in LTE transmission.

We propose a new antenna integration design, in which only one antenna is used. As a result, the space of mobile devices can be saved and the interference caused by different transmissions can be avoided.

Then, we study two scenarios based on different channels. Under the first scenario, a primary user and a secondary user transmit their own signals over the same AWGN channel. The simulation results indicate that by using a SIC scheme, an increasing system capacity can be obtained by the secondary transmission, with no sacrifice of the primary user's performance.

In the second scenario, the LTE and Wi-Fi transmit over a Rayleigh fading channel simultaneously. A straightforward estimation scheme is adopted to estimate the Channel State Information (CSI) at the receiver. We discuss two cases according to the CSI. The first case is that the CSI is available at the receiver. A novel scheme is proposed to overcome the disadvantages of a slow block fading channel. In this scheme, we implement an interleaver at both the transmitter and receiver, and therefore utilize the CSI efficiently at the receiver to improve the system performance. In the second case the CSI is available at both the transmitter and receiver. An adaptive power control scheme is proposed to adjust the transmitted power to a desired level, and therefore improve the system.

Acknowledgements

First and foremost, I would like to express my sincerest gratitude to my supervisor, Professor M. Reza Soleymani, for his patient guidance, encouragements, and general support during this research, and for giving me the opportunity to enjoy the happiness of the acquisition of knowledge in his group. Without his support and guidance, this thesis would not be presented today.

I would like to express my great thanks to all members of my Master defense committee: Dr. M. Z. Kabir , Dr. A. S. Ramamurthy and Dr. M. Mehmet-Ali . I greatly appreciate the suggestions, comments, and the time for reading this thesis.

I'm also thankful to all the colleagues in the Wireless and Satellite Communications Laboratory. Great thanks to Hesam Khoshnevis and Boulos Wadih Khoueiry, for sharing the knowledge without reservation.

Finally, more than anyone else, I would like to express my deepest gratitude to my lovely family - my parents and my cute girlfriend - for their endless love.

Contents

List of Figures	ix
List of Tables	xi
List of Abbreviation	xiii
1 Introduction	1
1.1 Motivation	1
1.2 Contribution	4
1.3 Thesis Outline	7
2 Background and Literature Review	8
2.1 Wireless Channels and Fading	9
2.1.1 Large-Scale Fading	9
2.1.2 Small-Scale Fading	11
2.2 Turbo Codes	12
2.2.1 Turbo encoder	14
2.2.2 Turbo decoder	15
2.2.3 BER performance of Turbo codes	18

2.3	LDPC Codes	20
2.3.1	Representations for LDPC codes	22
2.3.2	Regular and irregular LDPC codes	23
2.3.3	Decoding algorithms	23
2.3.4	BER performance of LDPC codes	25
2.4	Raptor Codes	27
2.4.1	Raptor encoder and degree distribution	28
2.4.2	Decoding algorithm	29
2.4.3	BER performance of Raptor codes	29
2.5	SIC: Successive Interference Cancellation	30
2.6	Adaptive Transmission	31
2.7	The Coexistence Status of LTE and Wi-Fi	32

3 System Model: Turbo and

Raptor Coded SIC with No

Channel State Information 35

3.1	Overview	35
3.2	System model under AWGN channel	37
3.3	Proposed Scheme: Successive Interference Cancellation Scheme . . .	38
3.4	Simulation Results	40
3.4.1	Simulation Parameters	40
3.4.2	Simulation Procedure	42
3.4.3	Simulation Results	42

4	Coexistence of LTE and Wi-Fi	47
4.1	Overview	47
4.2	Feasibility of the coexistence	48
4.2.1	LTE in the unlicensed bands	49
4.2.2	Download Booster	51
4.2.3	Feasibility	51
4.3	Antenna design of the coexistence of LTE and Wi-Fi	52
5	System Model: Turbo and Raptor Coded SIC with Channel State Information	55
5.1	Overview	55
5.2	System Model	57
5.3	Proposed Scheme	58
5.3.1	System over block fading channel with small memory size	59
5.3.2	System over block fading channel with large memory size	61
5.3.3	Adaptive power control scheme	62
5.4	Simulation Results	64
5.4.1	Simulation Results over block fading channel with a small memory size	65
5.4.2	Simulation Results over block fading channel with a large memory size	69
5.4.3	Simulation Results with adaptive power control scheme	73

6	Concluding Remarks	74
6.1	Conclusion	74
6.2	Future Work	77

List of Figures

2.1	Turbo encoder in 3GPP standard [1]	15
2.2	Turbo decoder	16
2.3	BER performance of Turbo code in terms of different iterations over AWGN channel with blocksize=2000 and rate=1/2	18
2.4	BER performance of Turbo code in terms of different block sizes over AWGN channel with 6 iterations and rate=1/2	19
2.5	BER performance of Turbo code in terms of different code rates over AWGN channel with blocksize=2000 and 6 iterations	19
2.6	Tanner graph representation of the parity check matrix	22
2.7	BER performance of LDPC code in terms of different block sizes over AWGN channel with iterations=30 and rate=1/2	25
2.8	BER performance of LDPC code in terms of different iterations over AWGN channel with blocksize=1024 and rate=1/2	26
2.9	BER performance of LDPC code in terms of different code rates over AWGN channel with iterations=30 and blocksize=1024	26
2.10	Raptor encoder	28

2.11	BER performance of Raptor code in terms of different code rates over AWGN channel with iterations=80	30
2.12	In-device coexistence[2]	32
2.13	Frequency division multiplexing for coexistence interference [2]	33
2.14	Time division multiplexing for coexistence interference [2]	34
3.1	System Model	38
3.2	Successive interference cancellation scheme	39
3.3	BER performance of Turbo code over AWGN channel versus nor- malized transmitted power	44
3.4	BER performance of system over AWGN channel with ratio=0.3	45
3.5	BER performance of Raptor code over AWGN channel with and without interference	45
4.1	Antenna Locations of Galaxy S5 [3]	52
4.2	The new design of antenna integration	53
5.1	System model over fading channel	57
5.2	Successive interference cancellation scheme with channel estimation	59
5.3	Successive interference cancellation scheme with an interleaver	61
5.4	Adaptive power control scheme	63
5.5	BER performance of the coexisting LTE and Wi-Fi transmissions over block fading channel with memory size=10, ratio=0.3	66
5.6	BER performance of the coexisting LTE and Wi-Fi transmissions over block fading channel with memory size=20, ratio=0.3	67

5.7	BER performance of single LTE transmission over block fading channel with memory size=10, ratio=0.3	68
5.8	BER performance of single LTE transmission over block fading channel with memory size=20, fading factor=0.3	69
5.9	FER performance of the coexisting LTE and Wi-Fi transmissions over slow block fading channel with no interleaver	70
5.10	BER performance of the coexisting LTE and Wi-Fi transmissions over slow block fading channel with interleaver size=1	71
5.11	BER performance of the coexisting LTE and Wi-Fi transmissions over slow block fading channel with interleaver size=10	72
5.12	BER performance of the coexisting LTE and Wi-Fi transmissions over block fading channel with memory size=10 and ratio=0.2 . . .	73

List of Tables

2.1 Path Loss Exponent for Different Environments	10
---	----

List of Abbreviation

3GPP	3rd Generation Partnership Project
ARQ	Automatic Repeat Request
AWGN	Additive White Gaussian Noise
BER	Bit Error Rate
BP	Belief Propagation
BPSK	Binary Phase Shift Keying
CRC	Cyclic Redundancy Check
CSAT	Carrier Sensing Adaptive Transmission
CSI	Channel State Information
CSMA/CA	Carrier Sense Multiple Access/Collision Avoidance
DVB-H	Digital Video Broadcasting-Handheld
DVB-RCS	Digital Video Broadcasting - Return Channel via Satellite
FDM	Frequency Division Multiplexing
FEC	Forward Error Correction
FER	Frame Error Rate
LBT	Listen Before Talk
LDPC	Low Density Parity Check

LLR	Log Likelihood Ratios
LOS	Line of Sight
LT	Luby Transform
LTE	Long-Term Evolution
LTE-U	LTE in Unlicensed Bands
LUT	Look-Up Table
MAP	Maximum <i>a posteriori</i>
MIMO	Multiple Input Multiple Output
ML	Maximum Likelihood
MMSE	Minimum Mean-Square-Error
MRD	Mobile Receive Diversity
MUI	Multi-User Interference
MUT	Multuser Transmission
NFC	Near field communication
OFDM	Orthogonal Frequency Division Multiplexing
PCCC	Parallel Concatenated Convolutional Code
RSC	Recursive Systematic Convolutional
SIC	Successive Interference Cancellation
SINR	Signal-to-Interference-plus-Boise Ratio
SISO	Soft Input Soft Output
SNR	Signal-to-Noise Ratio
TDM	Time Division Multiplexing
TDMA	Time-Division Multiple Access

UE	User Equipment
UMTS	Universal Mobile Telecommunications System
WLAN	Wireless Local Area Network

Chapter 1

Introduction

1.1 Motivation

As the demand for wireless communication increases in the present, we can be sure that the issue of utilizing bandwidth efficiently will be very important. High level modulation , pulse shaping, and Multiple Input Multiple Output (MIMO) techniques are deployed to drive the development of higher spectral efficiency. In the meantime, satisfying reliability under Multiuser Transmission (MUT) conditions, draws a lot of attention from the designers. In fact, the multiuser transmission or multiple access channel (MAC) is very difficult to conduct due to the interference caused by users in adjacent channels. In order to solve the adjacent channel interference issues, many techniques were proposed, such as Time Division Multiplexing (TDM), Frequency Division Multiplexing (FDM), and Power Control schemes [2], [4]. However, the problems are usually solved by sacrificing one user's benefit in terms of the quality of the transmission, and therefore the cost is

relatively high. On the other hand, the Successive Interference Cancellation (SIC) scheme motivates us to consider the possibility that multiple users transmit their signals in the same band simultaneously, which can utilize the bandwidth more effectively. There is a case where two systems transmit simultaneously. The two most significant ways to access the internet are Wi-Fi, which is usually deployed in the indoor environment and the other one is Long-Term Evolution (LTE), which is the main mobile standard in the world.

Error control coding schemes, on the other hand, are designed to improve the accuracy of the data recovery. Two broad categories, Automatic Repeat Request (ARQ) and Forward Error Correction (FEC) codes consist of error control coding schemes [5]. The ARQ method is a good way to make sure a stable performance of transmissions based on varying channels because it adapts to the channel. However, it is restricted to some transmission systems which need real-time information. As the feedback information from the receiver to the transmitter results in a lot of delay. On the other hand, FEC codes guarantee the performance of transmissions under the constant channel condition, but it is not adaptive in terms of different channel conditions. The rateless codes, such as Luby Transform (LT) codes [6] and Raptor codes [7], are a good way to solve this problem. The rateless codes advantages are combined both of ARQ and FEC codes. For each transmission, like other channel codes, both the transmitter and receiver encodes and decodes, respectively. However, the receiver will send a feedback to the transmitter and it is usually a very short message, to indicate whether the signal is decoded

correctly. The transmitter will send one more bit to the receiver to continue to decode the signal until the correct signal is obtained. By adding one bit for each re-transmission, the system gains a perfect performance at a really high code rate. It means that the number of coded symbols is only slightly larger than the number of data symbols. From another aspect, Turbo codes, as strong error correction codes, perform close to the Shannon limit [8] in terms of Bit Error Rate (BER). By using these codes, we guarantee the performance at a high level both for fixed and flexible rates. Some successive interference cancellation schemes using Turbo codes for wireless systems are proposed and examined in the formal literature [9], [10]. However, a wireless transmission system combining Turbo and Raptor codes by using SIC scheme for LTE and Wi-Fi, is rarely talked about. We take advantage of different channel codes in terms of the stable output of fixed code rate and the adjustable ability of flexible code rate at the same time. As Raptor codes are suitable for employing adaptive transmission schemes, transmitters can adjust the code rate in order to decode signals properly for the receivers to achieve a better performance.

Furthermore, antenna configuration is another main issue which concerns the hardware device designers. As we know, the space in mobile devices is very limited especially for smart phones. Usually, there are about 7 antennas integrated into one mobile device: two for 2.4 GHz and 5 GHz WLAN and Blue Tooth, one or two for LTE, one for GPS, one for Mobile Receive Diversity (MRD) and possibly one for Near field communication (NFC), and all need to be isolated from each

other in order to decrease the interference. Combining two antennas can trigger a huge influence on the signal transmission and the design of mobile devices.

1.2 Contribution

In this thesis, we propose the coexistence of LTE and Wi-Fi. We assume that both LTE and Wi-Fi will transmit simultaneously in the same band which seems to be unrealizable at the present. The standard of IEEE 802.11n is considered as the Wi-Fi standard. The transmission signal of Wi-Fi is assumed to be the stronger signal as Wi-Fi is usually configured in the indoor environment which does not experience large scale fading to cause a huge path loss. Meanwhile, the LTE signal which is the weaker signal in our system experiences the large scale fading and strong interference from the Wi-Fi signal. In order to decode both LTE and Wi-Fi signals correctly and efficiently, the successive interference cancellation scheme is applied in the source-destination transmission.

We implement a Raptor code for Wi-Fi which is discussed in [11] and [12], and the Turbo channel codes for LTE which is standardized in the 3rd Generation Partnership Project (3GPP). One reason for choosing Raptor codes for Wi-Fi is the advantages of rateless Raptor codes which is a perfect choice to recover the signal since the code rate can be adjusted to fit different channel situations. Besides, the Raptor codes perform well when there is an interference introduced and leads to the Signal-to-Interference-plus-Noise Ratio (SINR) to a relatively low level. On the other hand, the specification of Turbo codes is recommended in

[1], and the BER performance of Turbo codes achieved at a given Signal-to-Noise Ratio (SNR) is very close to Shannon's theoretical limit.

The factor of the fading channel is also considered. Two schemes are proposed for different situations based on the estimation of the Channel State Information (CSI), in order to recover the signals more accurately. An estimation scheme is adopted which has been proposed in [13], when the signal is transmitted over a block fading channel with a small memory size. There is a trade-off between the performance and the process complexity. The advantage of this new scheme is that the estimation process ends before the iterative decoding procedure with no pilot symbols. Therefore, it is a very straightforward process and saves a lot of time compared to other estimation schemes. Another scheme is proposed based on the block fading channel with a large memory size. This channel can be assumed as a channel with the fading coefficient remaining constant over one block. It is usually difficult to recover the original signal on account of the channel estimation information as there is not much diversity for decoder to decode over one block. An interleaver is implemented in our system to introduce more diversity. At the transmitter, the frames are sent to the interleaver before being transmitted. Then, at the receiver, the received frames are deinterleaved to rebuild original frames and passed to the decoder. By adding this interleaving process, the channel estimation information can be used for decoding more effectively.

The SIC scheme can be implemented not only over fading channel as we discussed previously, but also on the Additive White Gaussian Noise (AWGN) chan-

nel. Wireless channels without multipath can be represented as AWGN channel. We propose a system which can be used for these wireless transmissions. The SIC receiver will decode the stronger signal, re-encode and subtract it from the received signal. Finally, the weak signal can be obtained as though there is no interference. The SIC scheme is easily implemented over the AWGN channel because the channel introduces noise to the signal without any phase changing.

The configuration of antennas is a main consideration of our thesis. We deployed one antenna instead of two antennas of which one is for Wi-Fi, the other is for LTE to receive both signals simultaneously. By using one antenna, we can save some space in mobile devices. Space is a precious commodity in almost every mobile product.

Besides, an adaptive transmission power control scheme is considered to be deployed to achieve better performance. We first explore the scenarios where the power difference is fixed for both the main and interfering signals. The system combining the fixed code rate Turbo codes which can be punctured and flexible code rate Raptor code is tested. The Raptor codes with a flexible code rate has been shown in [7] and [14] to have an incredible capacity (performance), which is suitable to increase the efficiency and reliability of recovering the strong power signal under some interference circumstances. Based on the adaptive power control scheme, the power of the strong signal can be adjusted to adapt to the channel state. With the feedback of the CSI from the receiver to the transmitter, the power difference of the two signals is maintained at a desired level.

1.3 Thesis Outline

The remainder of the thesis will be organized as follows. In Chapter 2, we present a brief background for the main parts of the thesis on the wireless communication which includes fading environments, Turbo codes, LDPC codes, Raptor codes which are the representatives of rateless codes, successive interference cancellation scheme, and adaptive power control scheme. Along with background, the related literature is reviewed and different channel codes with simulation results are presented. In Chapter 3, we present the system model over an AWGN channel with no channel state information at the receiver, the strategy of choosing the simulation parameters, and the simulation results. Chapter 4 consists of the antenna structure of the coexistence of LTE and Wi-Fi system. In Chapter 5, we propose a system model over a fading channel deploying different estimation schemes along with an adaptive power control scheme. The simulation results are presented and will be compared with the results which are obtained with no channel state information and perfect channel state information. Finally, conclusions and suggestions for future work are discussed in Chapter 6.

Chapter 2

Background and Literature

Review

In this chapter, the background and literature review of related work to the proposed research are presented. We first introduce different kinds of fading in the wireless channels, which cause attenuation and delay when high data-rates information is transmitted in wireless environments. Then, different channel codes including Turbo codes, LDPC codes, LT codes, and Raptor codes are illustrated. After that, we present a transmission scheme which highly increases the efficiency of mutiusers' systems, the SIC scheme. Finally, we review the coexistence status of LTE and Wi-Fi after the brief introduction of the adaptive power control transmission scheme.

2.1 Wireless Channels and Fading

In the wireless communication systems, the accuracy of received signals compared with transmitted signals reveals the reliability of transmissions. The AWGN channels with different fading phenomenon consisting of the common wireless channels, are the media used to transmit signals. Among these propagation factors, the large-scale fading and small-scale fading are the main factors that affect the strength of the received signals. In the following section, we will explain these briefly.

2.1.1 Large-Scale Fading

The large-scale fading can be estimated by different parameters and models, such as the path loss and the log-normal shadowing. The path loss is usually defined as a drop in the received signal power as a function of distance in terms of different conditions. This function includes several parameters which are the transmitted signal power, system loss, and the distance between the transmitter and the receiver . The path loss exponent $d^{-\nu}$ is measured, in terms of distance depending on different circumstances, which describes the variation of received power. Therefore, the received signal power can be described as a function of the path loss exponent which is

$$P_r = P_t \frac{c}{d^\nu} \quad (2.1)$$

where P_r and P_t are the received power and transmitted power, respectively. c is a constant which includes wavelength, antennas' gain, and system loss. Based on different empirical models which are means for predicting the path loss, we have various path loss exponents in particular environments and are described in Table 2.1 [15].

Table 2.1: Path Loss Exponent for Different Environments

Environment	Path Loss Exponent, ν
Free Space	2
Urban area cellular radio	2.7 to 3.5
Shadowed urban cellular radio	3 to 5
In building line-of sight	1.6 to 1.8
Obstructed in building	4 to 6
Obstructed in factories	2 to 3

The predicted received signal power which is discussed above is the average signal power. In fact, measurements at different locations for a particular distance from the transmitter show a range of path loss values which lead the received power values around the mean of prediction. The shadowing from buildings, mountains, and other obstructions can cause the power changes to various positions of the receivers, however, they still remain the same distance from the transmitter. To account for the variations, Equation 2.2 is introduced as:

$$P_r |_{dB} = \bar{P}_r |_{dB} - l_{path} |_{dB} \quad (2.2)$$

where $\bar{P}_r |_{dB}$ is the average received signal power which can be obtained by Equation 2.1. $l_{path} |_{dB}$ is introduced by Equation 2.3 which describes the variations

around mean of path loss caused by shadowing:

$$L_{path}|_{dB} = \bar{L}_{path}|_{dB} + l_{path}|_{dB} \quad (2.3)$$

2.1.2 Small-Scale Fading

Being different from large-Scale Fading, small-scale fading is caused by multipath propagation. The signal can be reflected and scattered to introduce two or more transmission paths because of the buildings and other possible objects especially in urban environments. Each path may undergo a change in amplitude and a change in phase. Therefore, the receiver collects all the different signals that may lead to a significant change compared with the original signal. In addition, as each path may experience a different distance, the delays are introduced to the received signal.

The Rayleigh fading channel is one of the most significant models to estimate and calculate the amplitude and phase of the received signal for a real world environment. This channel can be applied to the urban environments without the line of sight. We use this model to establish a statistical system which represents the case of no direct line-of-sight path transmitted under urban environments.

As we mentioned above, the time delay of multipath signals from the first received signal to the last is one of the important characteristics of a fading channel, which is called delay spread. In frequency domain, the coherence bandwidth is defined as the reciprocal of delay spread. Based on the relation between the delay

spread and the transmitted signal duration, we define the flat fading and frequency selective fading. If the delay spread is much smaller than the signal duration, in other words, if the coherence bandwidth is considerably larger than the bandwidth of the signal, the fading channel is a flat fading channel. Otherwise the channel is called the frequency selective fading channel.

On the other hand, the Doppler spread is defined by different Doppler shifts and related to the coherence time. A Doppler shift emerges when a terminal is moving. Different Doppler shifts based on a multipath environment contribute to the Doppler spread. The coherence time is defined as the duration of the received signal level, which remains constant. Fast fading occurs when the signal duration is larger than the coherence time. Otherwise, the signal duration is smaller than the coherence time, which leads to the slow fading.

2.2 Turbo Codes

Approaching the Shannon limit is the core of wireless communications, which can be theoretically realized by adopting a large block length code or a convolutional code with usually a large constraint length. However, the complicated encoding and decoding process for long codes leads to the impossibility of practice.

A new class of convolutional codes solves this difficulty by combining the powerful encoder and decoder, called Turbo codes. Turbo codes play an important

role not only because they are one of the most powerful codes whose performance are close to the Shannon limit, but also as they are not too complicated to implement. In 1993, Turbo codes were first introduced by Berrou, Glavieux and Thitimajshima [16]. Since then, several schemes have been proposed to evaluate and increase the performance of Turbo codes, and so many researches and tutorials have been done in order to expand the implementation of these codes [17], [18], [19].

As we know, 3GPP Long Term Evolution [20] and LTE-Advance [1], [21] (4G network) provide much higher data rates, compared to 3G Universal Mobile Telecommunications System (UMTS). The high throughput of LTE-Advance, for instance, to provide up to 3 Gbps peak data rate [22], is extremely attractive and has led 4G to be deployed all around the world. According to the 3GPP standards [1], the Turbo codes are adopted and standardized for LTE transmissions.

The structure of typical Turbo codes, like other FEC codes, can be analyzed with an encoder and decoder separately. The Turbo encoder contains two parallel Recursive Systematic Convolutional (RSC) coders separated by an interleaver which generates short constraint length codes. The Turbo decoder consists of two iterative Soft Input Soft Output (SISO) decoders using the Maximum *a posteriori* (MAP) algorithm usually that looks for the most likely symbol received, which estimate the receive data more accurately. We will discuss each part briefly from different angles, algorithms, and processes in the following section.

2.2.1 Turbo encoder

A Turbo encoder is formed from parallel concatenation of two RSC coders, an interleaver, and a puncturing process. One RSC coder receives the input sequence, keeps it and generates a parity bits sequence. Meanwhile, the other RSC coder receives an interleaved version of the input sequence which is generated by the interleaver, and also generates a parity bits sequence. Afterwards, all the parity bits go into the puncturing process to increase the code rate. Finally, combining input sequence and the punctured parity bits sequence, the coded stream is transmitted to the decoder.

The interleaver plays an important role in the Turbo encoder because it serves two purposes of designing Turbo codes. Firstly, as is known, higher weight for codewords gives a better performance. For Turbo codes, the output of the second encoder is quite different from the first because the input to the second encoder is re-ordered. In other words, it is highly likely to generate the codewords that has high weight between two code generators, even though one of the codewords has low weight. Namely, the interleaver makes for a better performance of Turbo codes. In addition, if the decoder receives more information, the output of the decoder is closer to the source stream, which means the decoder can correct more errors. For this reason, the two Turbo encoders which generate different codewords by employing an interleaver give more information to decoders. Consequently, the interleaver is beneficial for the performance of the decoder. A pseudo-random interleaver is usually chosen in Turbo codes design compared to the "row-column"

interleaver, the "helical" interleaver, the "odd-even" interleaver, and so on [23], [24].

According to the 3GPP standards, the Turbo encoding scheme is a Parallel Concatenated Convolutional Code (PCCC) with two 8-state constituent encoders and one interleaver [1]. The Turbo coding rate is $1/3$, which means a set of triple bits are produced for every one source bit encoded. In order to increase the efficiency of the system, the code rate can be punctured to a higher rate [25], $1/2$ for example. The initial value of the shift registers of encoders will all be zeros when the encoders start to encode the input information bits. The block size of LTE has been defined from 40 to 6144. The structure of the turbo encoder is shown in Fig. 2.1.

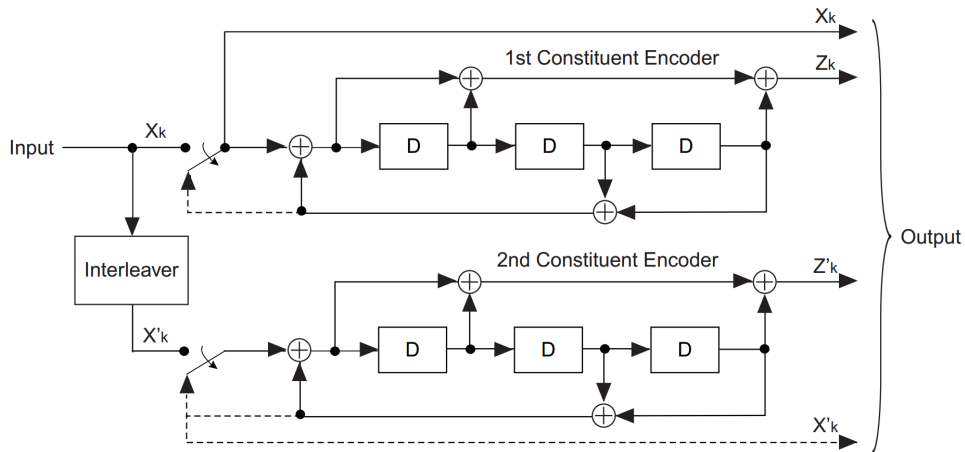


Figure 2.1: Turbo encoder in 3GPP standard [1]

2.2.2 Turbo decoder

The structure of a Turbo decoder is shown in Fig. 2.2. A Turbo decoder consists of a pair of decoders which exchange information with each other for the

sake of cycling the loops to calculate a stable and reliable value of each bit. SISO algorithms are introduced for iterative decoding as more information received from channels is sent to the decoder compared with hard input.

In order to calculate the final soft-output value, Equation 2.4 is introduced as:

$$L(\hat{u}) = L_c \cdot y + L_a(u) + L_e(\hat{u}) \quad (2.4)$$

where $L(\hat{u})$ is the *a posteriori* values for all information bits, namely soft-output value. L_c and y are the reliability values of the channel and the received information from the channel, respectively, where $L_c = 4 \cdot a \cdot R \cdot \frac{E_S}{N_0}$. For a Gaussian channel, $a = 1$; for a fading channel, a is the fading amplitude. In addition, R is the code rate. $L_a(u)$ is the *a priori* values for all information bits, and the extrinsic value is $L_e(\hat{u})$.

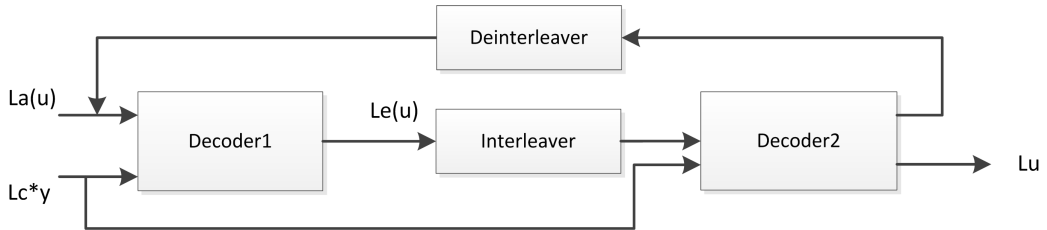


Figure 2.2: Turbo decoder

Based on the Fig. 2.2 and Equation 2.4, the process of Turbo decoding can be described briefly as follows. Initially, the first decoder begins with no *priori* information available, in which $L_a(u)$ is equal to zero. According to the channel values $L_c \cdot y$, we can calculate the extrinsic value L_e^1 , which is the *a priori* value to the second decoder after passing an interleaver. Then, the second decoder deals

with these values in the same way. For a predefined number of iterations, the extrinsic values of these two decoders are always updated. Finally, the estimate of the soft-output value can be achieved.

The Max-Log-MAP algorithm is one of the suboptimal MAP algorithms but without the MAP algorithms' major disadvantages, because the Max-Log-MAP algorithm is easier to implement. By computing Log Likelihood Ratios (LLR) values for each bit according to the given values of received bits and information which is collected from the forward and backward recursions, the decoder gives us the most probable value for each received bit which is either 1 or 0 for the Binary Phase-Shift Keying (BPSK) modulation. The LLR values $L(\hat{u})$ for each bit can be computed in Equation 2.5 according to the collected information α_k and β_k from the forward and backward recursions in Equation 2.6 and 2.7 as follows:

$$L(\hat{u}_k) = \max_{u_k=1} \{\alpha_{k-1}(s_{k-1}) + \gamma_k(s_{k-1}, s_k) + \beta_k(s_k)\} \\ - \max_{u_k=-1} \{\alpha_{k-1}(s_{k-1}) + \gamma_k(s_{k-1}, s_k) + \beta_k(s_k)\} \quad (2.5)$$

$$\alpha_k(s_k) = \max_{s_{k-1}} \{\alpha_{k-1}(s_{k-1}) + \gamma_k(s_{k-1}, s_k)\} \quad (2.6)$$

$$\beta_k(s_k) = \max_{s_{k+1}} \{\beta_{k+1}(s_{k+1}) + \gamma_k(s_k, s_{k+1})\} \quad (2.7)$$

The γ_k term above is the branch transition probability which is defined as follows:

$$\gamma(s_{k-1}, s_k) = \frac{1}{2}L_c \cdot y_{k,1} \cdot u_k + \frac{1}{2}L_c \cdot y_{k,2} \cdot x_{k,2} + \frac{1}{2}u_k \cdot L(u_k) \quad (2.8)$$

where L_c is the reliability value of the channel, $y_{k,1}$ and $y_{k,2}$ are the received message bits and check bits, respectively. The details of The Max-Log-MAP algorithm are given in [5], as well as all needed equations.

2.2.3 BER performance of Turbo codes

The performance of the Turbo codes can be evaluated by plotting BER vs. SNR and depends on various parameters: the decoding algorithm, the type of interleaver, the number of iterations, the block size, and also the code rate. The simulation results are illustrated in Figures 2.3, 2.4, and 2.5. The modulation is BPSK and the channel is AWGN channel.

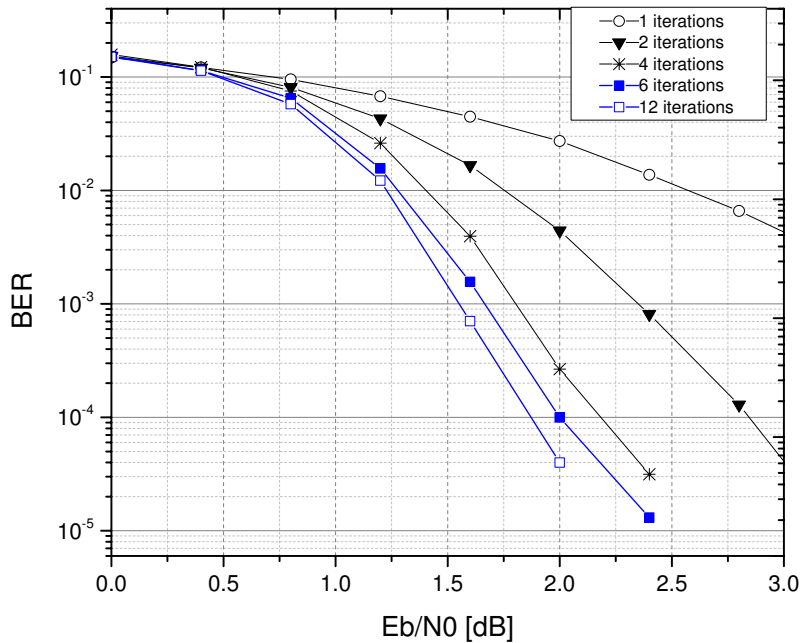


Figure 2.3: BER performance of Turbo code in terms of different iterations over AWGN channel with blocksize=2000 and rate=1/2

In Figures 2.3, 2.4, and 2.5, the simulation results of different iterations, block sizes, and code rates are compared, respectively. The simulation results show that

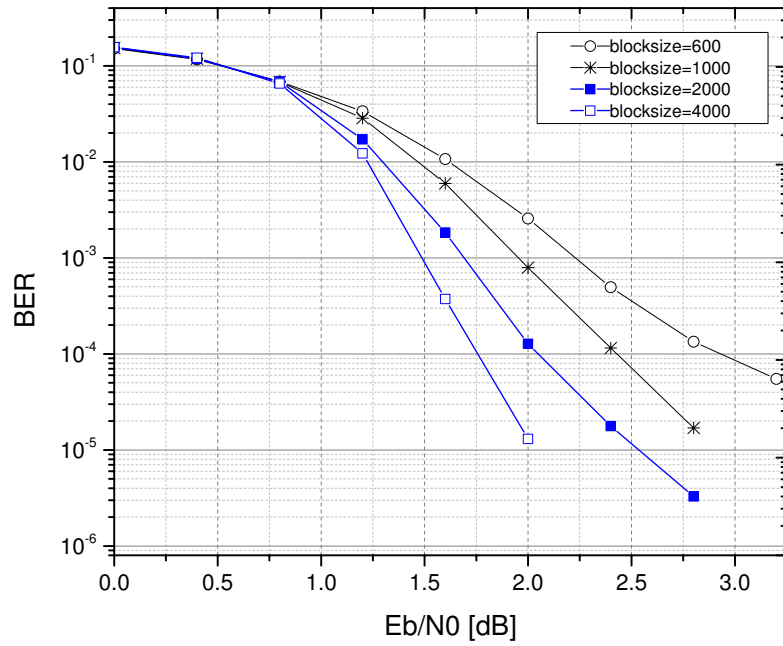


Figure 2.4: BER performance of Turbo code in terms of different block sizes over AWGN channel with 6 iterations and rate=1/2

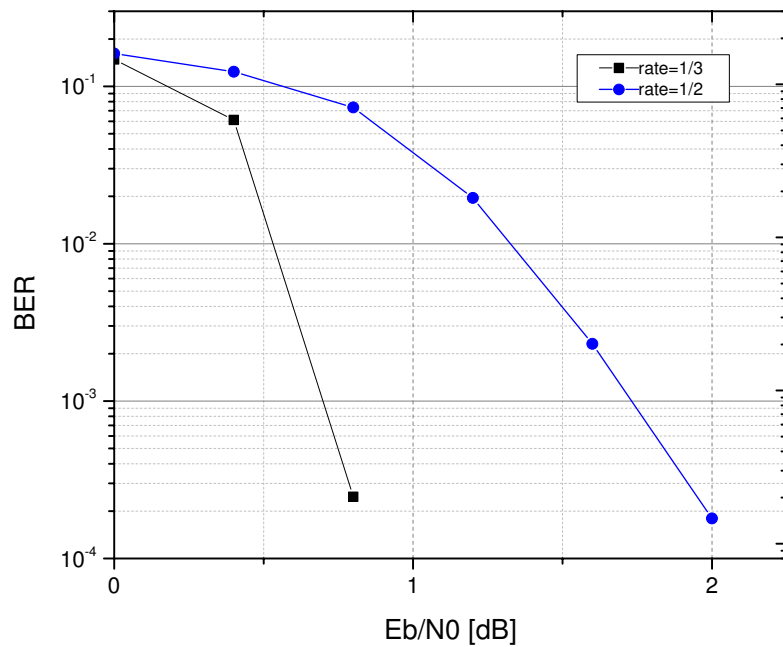


Figure 2.5: BER performance of Turbo code in terms of different code rates over AWGN channel with blocksize=2000 and 6 iterations

the BER performance gets better as the iteration and block size increase and the code rate decreases. However, one thing needs to be emphasized and illustrated. Fig. 2.3 shows the influence upon the performance caused by the number of iterations. According to the same SNR, the performance with a larger number of iterations is better than one with smaller number. However, after 6 iterations, the increasing number of iterations cannot lead to an obvious better result. In the meantime, the more iterations that are set, the more process time is needed. Therefore, it can be concluded that 6 iterations is a perfect choice to simulate Turbo codes.

2.3 LDPC Codes

Low Density Parity Check (LDPC) codes, which were first proposed by Gallager [26], are another type of forward error-correction codes different from the Turbo codes which we discussed above. As we know, the decoding complexity of one kind of FEC codes determines whether it is just at the theoretical level or suitable for implementation for the most part. From this perspective, as their name suggests, LDPC codes are designed to contain a very small number of non-zero factors in the parity-check matrices. Therefore, LDPC codes drew a lot of attention again after a few decades.

We not only get good performance from the LDPC codes, but the codes are also a fundamental part of Raptor codes. This motivates us to investigate them. As mentioned earlier, a sparse parity-check matrix which the name low-density

parity-check codes comes from, represents the density of the LDPC matrix. When the length of the codes goes to infinity, the density is almost zero.

In order to be familiar with LDPC codes, we should pay particular attention to the decoder design, because a sparse parity-check matrix is first constructed for the sake of complexity. The decoding process, by using such as message-passing algorithms, is dependent on the sparse parity-check matrix since it provides a solution to form a Tanner graph to decode signals properly. Generally, it is not practical to look for a sparse parity-check matrix based on an existing codeword. Accordingly, a generator matrix is introduced on the strength of the parity-check matrix.

Compared with Turbo codes, there are some advantages of LDPC codes that need to be illustrated. Unlike Turbo codes, the parity-check matrix makes sure the decoding process for LDPC codes can be terminated early before running the whole round of iterations which are already set up for the decoder. By computing the output of the decoder with the parity-check matrix in each iteration, the result reveals whether a valid codeword is obtained or if the decoder should run another iteration. In both simulations or practical circumstances, it will save a lot of time if the decoder is dynamic to deal with the received information from the channel and determine the time to stop. In addition, the LDPC codes do not need an interleaver. An interleaver's size increases with the length of the codeword. For long codes, this leads to a long delay at both transmitter and receiver sides.

2.3.1 Representations for LDPC codes

There are two major different ways to represent LDPC codes. One is the matrix representation based on a sparse parity-check matrix like other linear block codes.

The other is a graphical representation, such as the Tanner graph.

$$H = \begin{bmatrix} 1 & 0 & 0 & 1 & 1 & 0 \\ 1 & 1 & 1 & 0 & 0 & 0 \\ 0 & 0 & 1 & 0 & 1 & 1 \\ 0 & 1 & 0 & 1 & 0 & 1 \end{bmatrix} \quad (2.9)$$

There is a matrix example shown in Equation 2.9 with parity check matrix for a (6,4) code. We define w_r for the number of 1's in each row and w_c for the number of 1's in each column, where w_r and w_c should be much smaller than the size of a matrix in terms of a matrix to be called low-density.

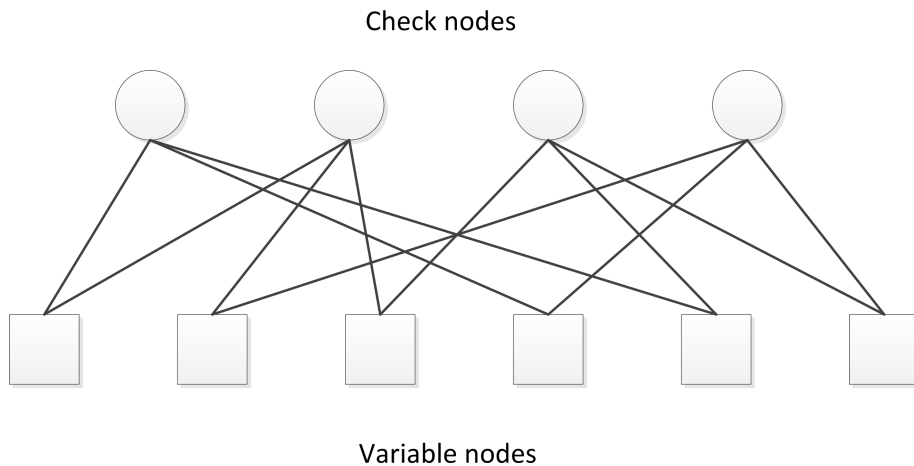


Figure 2.6: Tanner graph representation of the parity check matrix

Fig. 2.6 shows another method to illustrate LDPC codes which is the Tanner graph. It provides two different types of connecting nodes which are variable

nodes and check nodes. Correspondingly, variable nodes represent the number of message bits in a codeword and check nodes represent the number of parity bits.

2.3.2 Regular and irregular LDPC codes

Usually, there are two kinds of LDPC codes for the sake of the structure of the matrix, which are regular and irregular LDPC codes. The former codes have the parity check matrix that w_c is constant and w_r is also constant according to the number of rows and columns. From Equation 2.9, for instance, we can see it is a regular LDPC code with $w_c = 2$ and $w_r = 3$. From another point of view, it is shown in the Tanner graph that same type of node contains the same number of edges which we can see from Fig. 2.6. The second codes, on the contrary, the number of 1's is not constant and it is usually generated randomly. [27] shows that the performance of irregular LDPC codes is better than regular LDPC codes.

2.3.3 Decoding algorithms

The message-passing algorithms are one of the most important algorithms used to decode LDPC codes. Based on a Tanner graph, messages received from a channel are passed between variable nodes and check nodes.

Bit-flipping algorithm [28] is one kind of message-passing algorithms in terms of hard decision before decoding. The messages passed along the edges are binary bits. Then, each node calculates the result based on the received messages from other connected nodes. The decoding process will be halted if all the parity-check

equations are satisfied according to the result from each node or if it reaches the maximum number of iterations that is settled in advance. Based on the hard decision before decoding, we lose some information from the channel.

Another one is the Belief Propagation (BP) algorithm, also called sum-product algorithm. It is a soft decision message-passing algorithm that keeps the information collected from the channel and transfers the probability of each received bit as *a priori* value. As the Max-Log-MAP algorithm of the Turbo codes we discussed before, the sum-product algorithm also can be evaluated by computing *a priori* probabilities $L(c_i) = 4 \cdot a \cdot R \cdot \frac{E_s}{N_0}$ and *a posteriori* probabilities $L(Q_i)$, where a is the fading amplitude and R is the code rate. Equations 2.10, 2.11, and 2.12 are introduced in terms of *a priori* and *a posteriori* probabilities:

$$L(r_{ij}) = 2 \operatorname{atanh} \left\{ \prod_{i' \in V_j \setminus i} \operatorname{tanh} \left[\frac{1}{2} L(q_{i'j}) \right] \right\} \quad (2.10)$$

$$L(q_{ij}) = L(c_i) + \sum_{j' \in C_j \setminus j} L(r_{j'i}) \quad (2.11)$$

$$L(Q_i) = L(c_i) + \sum_{j' \in C_j} L(r_{j'i}) \quad (2.12)$$

We rewrite these equations in this way based on [28] in order to simplify and show the process directly. In order to perform fast iterative decoding over the AWGN channel, two simplified methods of the belief propagation algorithm are proposed in [29]. These two new algorithms show a good performance in terms of the lower complexity.

2.3.4 BER performance of LDPC codes

In this thesis, a (3,6)-regular LDPC code is chosen for simulation. The performance of the LDPC codes is evaluated by plotting BER vs. SNR and we use the different number of iterations, the block size, and also the code rate to compare the simulation results which are illustrated in Figures 2.7, 2.8, and 2.9. The modulation is BPSK and the channel is AWGN channel.

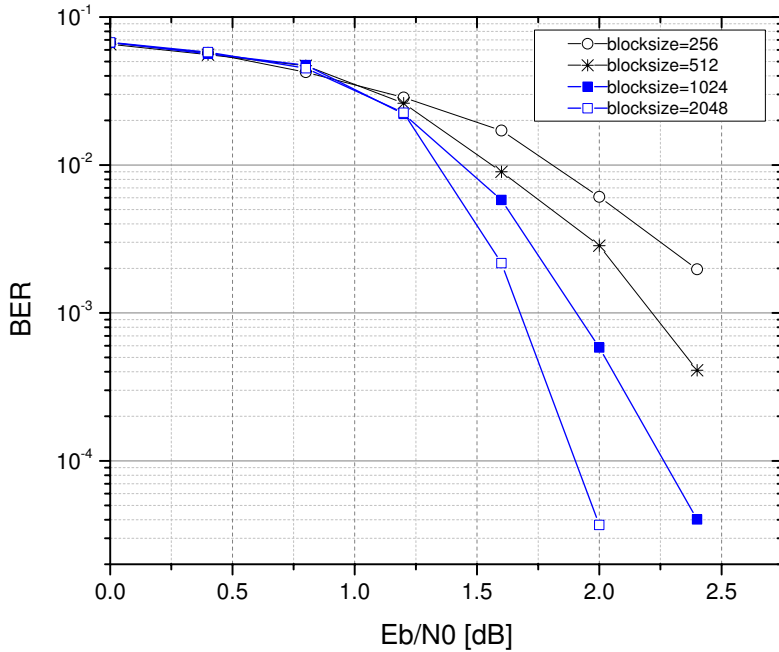


Figure 2.7: BER performance of LDPC code in terms of different block sizes over AWGN channel with iterations=30 and rate=1/2

The simulation results reveal that the performance of LDPC codes gets better as the block size increases and the code rate decreases. Also, we need to pay attention to the selection of the number of iterations in the decoder. It can be observed that after 50 iterations, the benefit we achieve from the increase in the number of iterations is relatively small compared to the gain we get from 20 iterations to 50

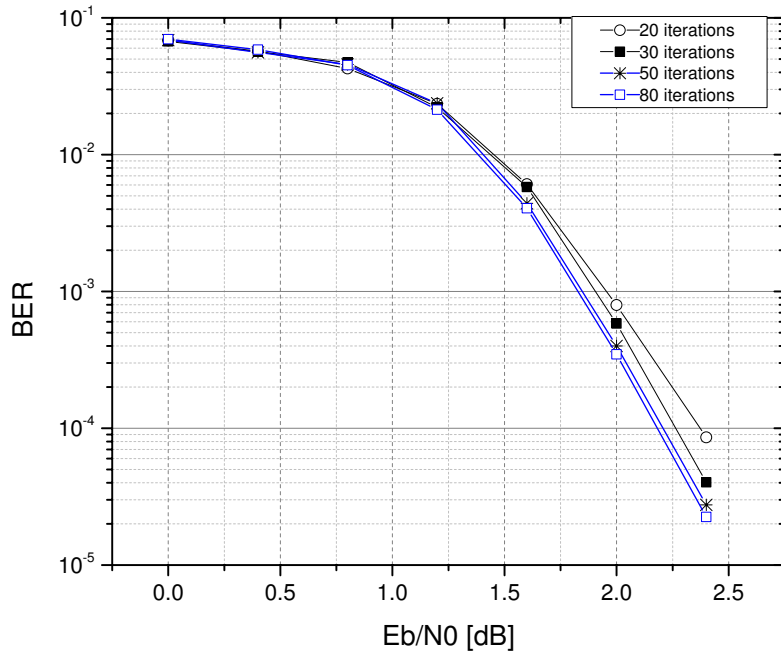


Figure 2.8: BER performance of LDPC code in terms of different iterations over AWGN channel with blocksize=1024 and rate=1/2

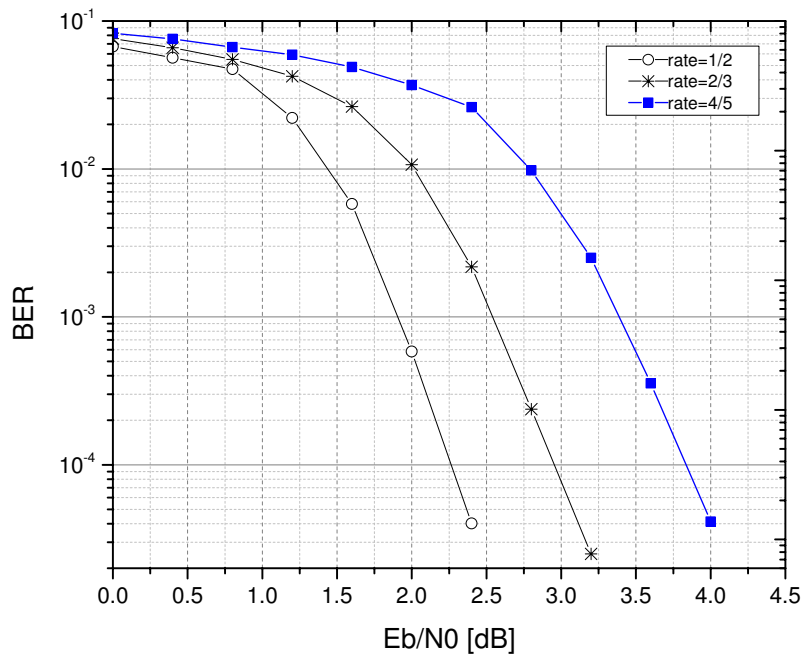


Figure 2.9: BER performance of LDPC code in terms of different code rates over AWGN channel with iterations=30 and blocksize=1024

iterations. Therefore, 50 to 80 iterations could be a perfect selection for LDPC codes.

2.4 Raptor Codes

Unlike the Turbo codes and LDPC codes, Raptor codes are one of the fountain codes which are rateless channel codes with a non-constant rate. The number of coded symbols is only slightly larger than the number of data symbols, and therefore a high code rate is usually guaranteed.

The fixed-rate channel codes are based on one channel condition to design. Therefore, the codes would result in decoding failure when the channel condition goes bad; on the other hand, the extra unnecessary symbols will be transmitted if the channel condition goes good. This leads to a disadvantage that either the transmission fails if the code rate is underestimated or the bandwidth is wasted if it is overestimated.

In order to solve this problem, one solution was proposed to have the channel state information at the transmitter. However, the channel estimation scheme needs to be performed and a low-rate feedback channel from the receiver to the transmitter will be needed. These requirements lead to more complexity and a larger delay. Recently, LT codes were introduced by Luby [6] as another solution. The codewords are generated in terms of a probability distribution which is optimized in [30]. However, the error floors of LT codes [31] cause the unfixed

encoding cost, and therefore motivate the use of an outer code which leads to the introduction of the Raptor codes. Raptor codes, by adding a high code rate LDPC code, overcome these difficulties and problems of LT codes and the solution with CSI at the transmitter. The Raptor codes can achieve a good performance without complete CSI. This means it is an advantage when the channel state information is unknown. The channel quality is not stable in a realistic application. Therefore, the system deploying rateless codes, such as Raptor code, becomes adaptive.

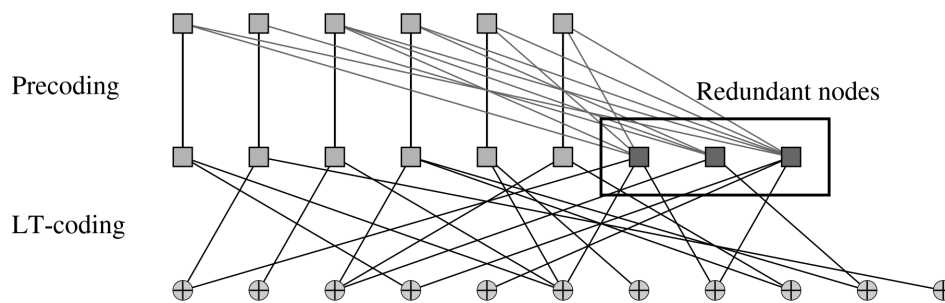


Figure 2.10: Raptor encoder

2.4.1 Raptor encoder and degree distribution

As it is shown in Fig. 2.10, the Raptor encoder is usually the combination of two channel codes with LT codes as inner codes and LDPC codes as outer codes. According to a degree distribution, the encoder continues to generate transmitter symbols based on the source symbols until the receiver is able to decode the signals successfully. For each transmission, the transmitter will only send one more bit to the receiver to continue to decode the signal until the correct signal is obtained. By adding one bit for each re-transmission, the system gains a perfect performance.

Degree distribution draws a lot of attention especially for different lengths of codewords. [7] optimized a degree distribution for the length of 63,358 bits which means the long codeword can achieve a good performance. However, there are rare optimized distributions for short codes. [32] and [33] present distributions that have been verified to have a relatively good simulation result. Choosing a degree distribution is a trade-off between excellent performance and decoding complexity. In our system, the distribution in [34] is selected for simulation. According to this paper, this distribution is optimized for Raptor codes with short length codewords. The highest degree is chosen as 33, which means the most connected nodes in the LT code layer is 33 nodes. As a result, the complexity of the system is decreased and the performance maintains a relatively high level in the meantime.

2.4.2 Decoding algorithm

A Raptor decoder which is deployed by using a soft decoding algorithm can be separated into two BP decoders. For the LT layer, the decoding algorithm is almost the same as the LDPC soft decoding algorithm. In [35], the details of both the hard and soft decoding algorithms of LT codes for wireless broadcast including the calculating formulas are introduced and some simulation results under the AWGN and fading channels are given.

2.4.3 BER performance of Raptor codes

As a rateless code, the code rate of each transmission is usually not fixed. In order to compare the performance of Raptor codes with other channel codes

we simulated above, the fixed-overhead codes are selected for simulation. The performance of the Raptor codes is also evaluated by plotting BER vs. SNR. As we presented the performance of different iterations for LDPC codes previously, and LDPC codes are one of the two layers of Raptors codes, we already have a concept of the effect on different iterations. At this point, we do not compare different iterations anymore. The different code rate is used to compare the simulation results which is illustrated in Fig. 2.11. The modulation is BPSK and the channel is AWGN channel.

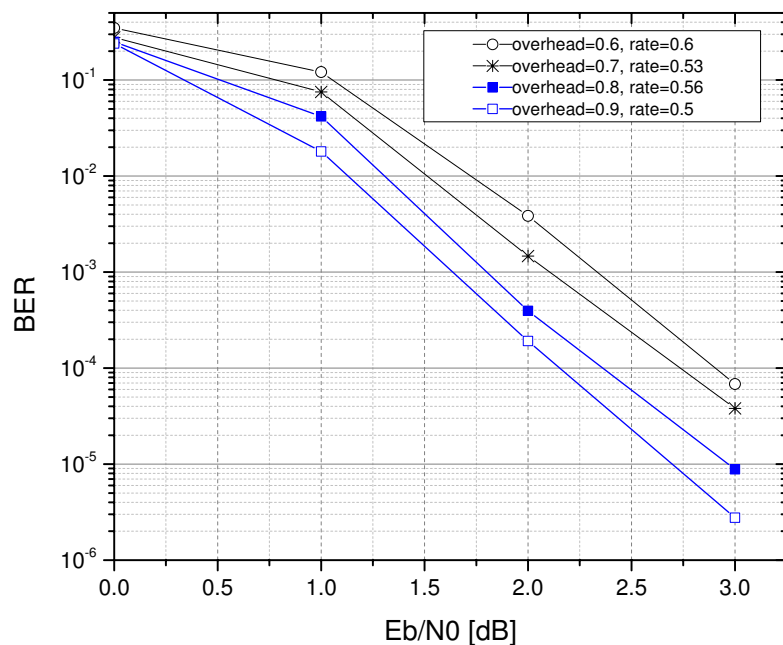


Figure 2.11: BER performance of Raptor code in terms of different code rates over AWGN channel with iterations=80

2.5 SIC: Successive Interference Cancellation

It is common that TDM or FDM is adopted in multi-user transmissions, which means multi-users cannot transmit their signals in the same band simultaneously.

The reason why we usually use these schemes is the huge Multi-User Interference (MUI) caused by other users' transmissions in the same slot cannot be taken care of well. The SIC scheme [36] [37], to the contrary, decreases the effect of MUI and increases the throughput of a channel by employing a multiple power system.

The SINR is the most important parameter for SIC to decode each user's signal correctly. When the highest SINR of one signal is larger than some point, the signal can be decoded correctly, then the signal will be re-encoded and subtracted from the original received signal. The process continues until all users' signals are distinguished. An attractive aspect is that one transmission at some proper power level will not be affected by other transmissions as long as the others can be decoded successfully.

2.6 Adaptive Transmission

In order to maximize the throughput under specific channel situations, adaptive transmission is introduced if the CSI is available from transmitter to receiver. Not only for single transmission, but also for multi-user transmissions, the transmitter can adjust transmitting parameters itself based on the power adaptation scheme, rateless channel coding, and modulation adjustment to optimize the transmission condition for the sake of the efficiency and accuracy.

Power control scheme (or power adaptation scheme) is one of the most direct method to adjust transmission with CSI. If the channel condition is good, the

signal is transmitted with proper power instead of maintaining the maximum transmitted power; otherwise, we increase the power to overcome the effect of the undesirable channel condition. From another point of view, rateless codes give us a possibility to adapt transmission environments by changing the code rate. With no complete CSI, the Raptor codes generate one extra symbol for each transmission until the the signal is decoded successfully.

2.7 The Coexistence Status of LTE and Wi-Fi

Nowadays, the LTE and Wi-Fi systems deploy different bandwidth and the terminal devices contain both the LTE and Wi-Fi receivers. These two systems cannot transmit in the same band simultaneously, which is very inefficient for using the limited bandwidth, and therefore inconvenient for users.

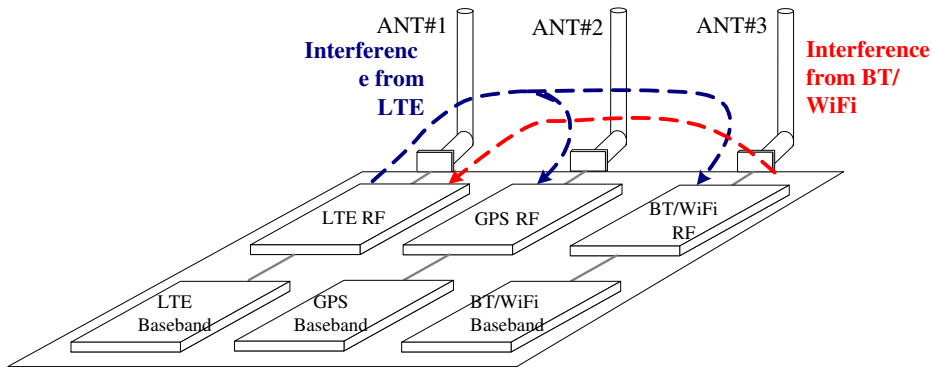


Figure 2.12: In-device coexistence[2]

With the limitation of the available bands and the increasing requirements of users, a new system needs to be proposed so that the LTE and Wi-Fi are deployed in the same band and the integration of these two receivers in the same User Equipment (UE) is required which indicates the in-device coexistence. However,

these two systems can cause significant interference to each other.

Recently, the 3GPP organization focused on the signaling and procedure for in-device interference avoidance. Three main solutions (e.g., the frequency division multiplexing, the time division multiplexing, and the power control) are proposed [2], which are illustrated in Figures. 2.12, 2.13, 2.14. Based on that, the amount of research effort is towards the interference detection [38], effect [39] and avoidance [4], [40] in adjacent channels.

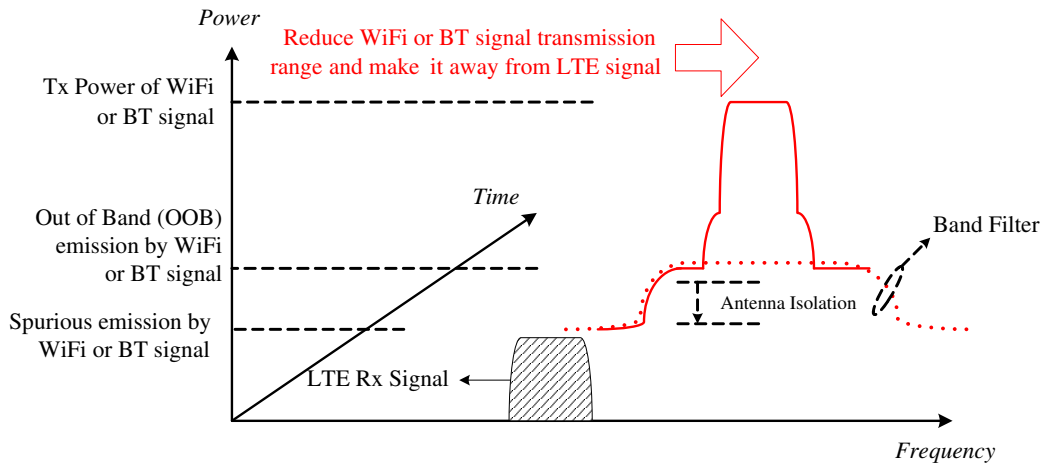


Figure 2.13: Frequency division multiplexing for coexistence interference [2]

However, if the LTE and the Wi-Fi need to transmit in the same band simultaneously or the need of a new method to take care of the overlap caused by adjacent bands transmission, the schemes and solutions which are mentioned above cannot be deployed in such scenarios. Therefore, a new system allowing two complete systems to simultaneously operate in the same frequency band is necessary.

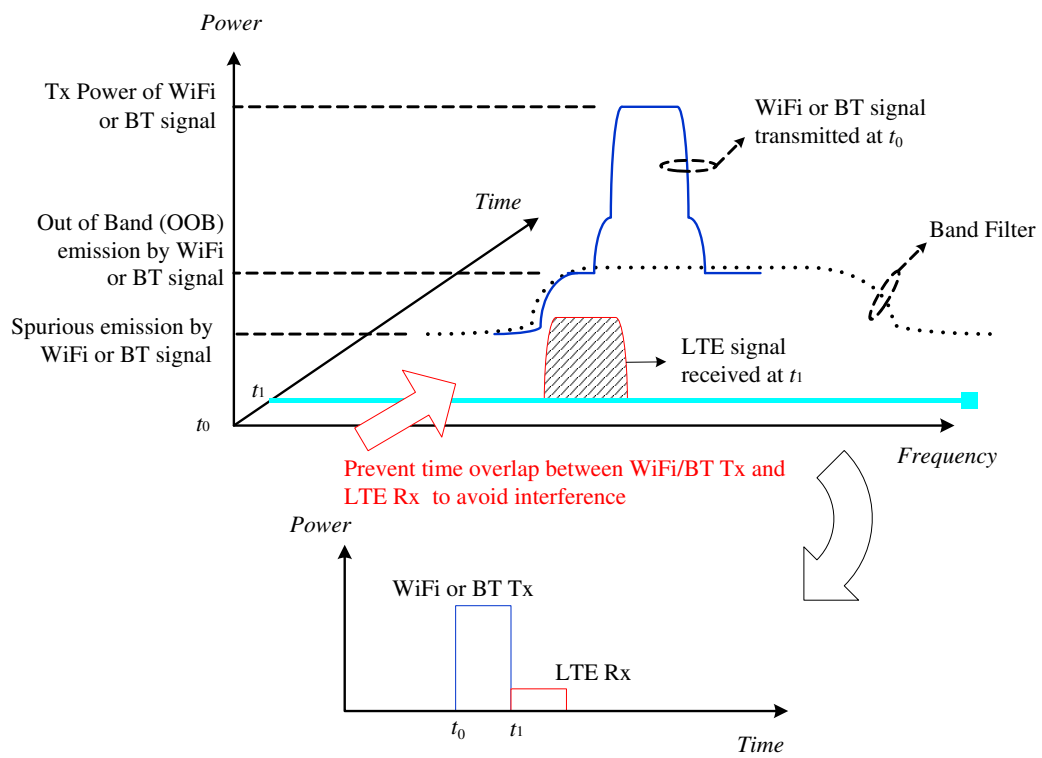


Figure 2.14: Time division multiplexing for coexistence interference [2]

Chapter 3

System Model: Turbo and Raptor Coded SIC with No Channel State Information

3.1 Overview

In this chapter, the coexistence between the transmissions of a primary user and a secondary user over the same AWGN channel is proposed. The primary transmitter is the main source and the secondary transmitter is an interfering source, share the same channel with no CSI at the receiver. The receiver is a UE deploying an effective SIC scheme. As DVB-RCS or a fixed, LOS wireless channel transmission can be reasonably assumed to be under an AWGN channel [41], the scheme we propose in this chapter can be applied for increasing the capacity of the overall system.

In order to increase the channel capacity, a number of methods have been proposed recently, such as MIMO techniques and relay cooperation systems. However, these usually cannot respond to the unexpected changes by merely adjusting the code rate once the hardware structure of a system is determined, because the fixed rate channel codes are adopted by these methods and they are not adaptive. Rateless codes, such as Raptor codes, on the other hand, overcome this shortcoming by means of the adjustment of code rate adaptively. This is an enormous advantage especially when a user as an interference intervenes in the existing transmission channel with no CSI of the channel in operation. Moreover, the Raptor codes are suggested for use in many wireless transmission standards, such as 3GPP standards for use in mobile cellular wireless broadcast and multicast [42], and also the DVB-H standards for IP datacast to handheld devices [43].

The transmission from the secondary transmitter to UE as interference adds to the existing main link. In such a case, the channel will be shared by two sources. In order to increase the overall throughput, the SIC scheme is adopted here. In our system, one of the attractive aspects is that introducing the interference channel does not affect the main source transmission, and as a consequence needs no adjustment to the main channel.

Power level difference is one of the concerns in our system. When the two signals have the same power level, we will have a binary erasure channel which is discussed in [44]. When the different symbols are sent from different sources, they will cancel out each other. Therefore, the channel capacity equals to 0.5 where we

consider the probability of each received symbol. Moreover, a probability of 0.5 may occur to a decision where the received bits equal to transmitted bits or if it is an error. The simulation results are illustrated in [45]. According to this, it is better to maintain a power difference between the two sources in our system.

3.2 System model under AWGN channel

In our model, the main source stream is transmitted from primary source S_1 to the destination D over an AWGN channel. The secondary source S_2 , as interfering source, transmits its own stream to the same destination D over the same channel. According to the characters of AWGN channel, it is applicable to DVB-RCS transmission [46] or a fixed, LOS wireless channel. Both transmitters are assumed to be symbol-synchronized and therefore the streams can be decoded frame by frame. In order to represent and calculate the receive signal y , Equation 3.1 is introduced as:

$$y = \sqrt{P_1} \cdot x_1 + \sqrt{P_2} \cdot x_2 + z \quad (3.1)$$

where P_1 and P_2 are the energy per bit for the main source and interfering source, respectively. We define the codeword x_1 and x_2 where $E[x_1^2] = E[x_2^2] = 1$, and z is a Gaussian random vector with zero mean and $\frac{\sigma^2}{2}$ variance.

The interfering source power P_2 is assumed larger than the main source power P_1 , where $P_2/P_1 \gg 1$. The successive interference cancellation scheme is used in

our system to maintain the power level difference needed.

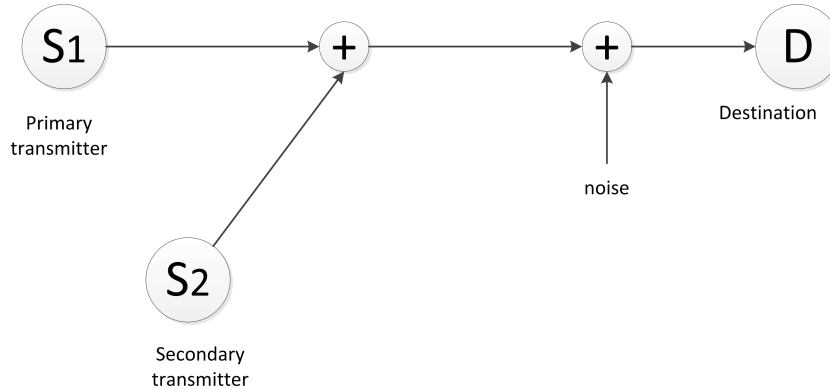


Figure 3.1: System Model

The system model is illustrated in Fig. 3.1. The primary source and the secondary source transmit their own signals on the same band simultaneously. After adding noise, the destination receives both streams as the whole signal y . It will first feed the signal to the secondary decoder to decode because the power of the interfering signal is higher than the other. After decoding successfully, the main source signal can be decoded by re-encoding and subtracting the interfering signal. According to the proposed scheme, the primary source signal can be obtained as though there is no interfering streams being transmitted.

3.3 Proposed Scheme: Successive Interference

Cancellation Scheme

Assuming that the secondary transmitter has data streams needed to send, in the meantime, the channel is occupied by primary transmission which cannot be interfered. According to the cognitive radio network [47] [48], the secondary user

needs to sense and detect the channel first to find the blank holes. Then, the stand-by data streams are filled into these holes to utilize the bandwidth more efficiently. There are two problems that need to be considered. One is the time cost of the sensing procedure and the misdetection possibility, both will lead a delay of the system and inefficient transmission. The other problem is the sensing error possibility which leads a huge interference to the main source and it is not acceptable. Except this cognitive radio scheme which drew a lot of attention recently, the solutions in [2] that we mentioned previously also introduce all kinds of problems.

Compared with other schemes, there are some advantages of the SIC scheme we propose to improve the system more efficiently. The core of this system is a consecutive integrated decoder. The procedure is shown by Fig. 3.2 in detail.

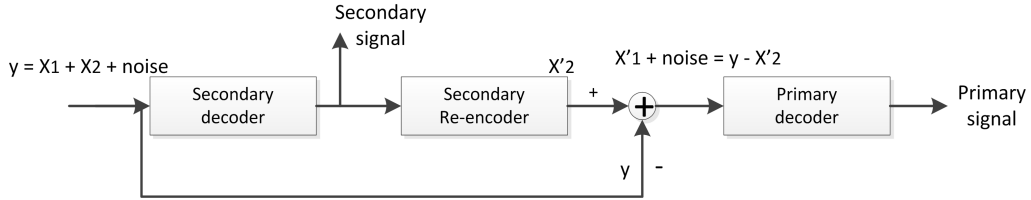


Figure 3.2: Successive interference cancellation scheme

The main source signal X_1 is transmitted from the primary transmitter using Turbo codes. At the same time, the secondary user arranges its own signal X_2 stand-by to be transmitted on the same channel, which is encoded by Raptor codes.

The receiver then performs the SIC scheme. The received signal y is sent to the secondary decoder first, which is for Raptor codes. As the power level of interfering signal X_2 is higher than the main source signal X_1 , it is easy to decode the signal based on power difference. Here, the main source signal X_1 is the interfering signal to the decoder and does not introduce a noticeable effect. After passing the decoder, the successful decoding signal is re-encoded to generate a new signal X_2' and we can assume X_2' is equal to X_2 . The main source signal X_1 with noise can be obtained by subtracting X_2' from the received signal. Then, the primary Turbo decoder decodes the rest of the signal which is the same as point to point transmission because there is no more interference.

3.4 Simulation Results

3.4.1 Simulation Parameters

In our simulations, the primary user chooses Turbo codes as its channel codes and the Raptor codes are selected to guarantee the transmission of the secondary user. We consider an AWGN channel, where the standard deviation for the noise is chosen to be $\sigma = \sqrt{0.5}$. The modulation scheme is chosen to be BPSK for the sake of simplicity and can be adjusted to high modulations as needed.

The configuration of Turbo codes is based on the 3GPP standard as we mentioned previously and can be replaced by LDPC codes as specified in the DVB-RCS standard. A PCCC with two 8-state constituent encoders and one interleaver has

been chosen as a Turbo encoder and the coding rate is 1/2 which is punctured via a puncturing process and can be punctured to other code rates as needed according to different choices of interleavers and processes. The Max-Log-MAP algorithm is selected in the Turbo decoder in our simulations and the number of iterations is fixed at 6.

There are two layers of Raptor codes which are LT codes as inner codes and LDPC codes as the pre-code. For the pre-code, a rate 0.95 (3,6)-regular LDPC code has been chosen in our simulations. This high rate code ensures the encoding cost at a fixed level. For the inner code, the degree distribution $\Omega_l(x)$ has been proposed in [7]

$$\begin{aligned} \Omega_l(x) = & 0.008x + 0.49x^2 + 0.166x^3 + 0.072x^4 + 0.083x^5 \\ & + 0.056x^8 + 0.037x^9 + 0.056x^{19} + 0.025x^{66} + 0.003x^{67} \end{aligned} \quad (3.2)$$

However, this distribution is optimized for codewords 65,536 bits long. If the short length codeword needs to be simulated, we have to look for a new optimized degree distribution. In [34], the improved degree distribution Ω_s is optimized for a short length codeword and shows a good performance:

$$\begin{aligned} \Omega(x) = & 0.03299x + 0.49357x^2 + 0.16722x^3 + 0.07265x^4 + 0.08256x^5 \\ & + 0.05606x^8 + 0.03723x^9 + 0.05559x^{19} + 0.003135x^{33}. \end{aligned} \quad (3.3)$$

The BP decoding scheme is employed for both decoders with 50 iterations and 80 iterations for LDPC codes and LT codes, respectively. A better result can be

achieved by increasing the number of iterations for both codes.

3.4.2 Simulation Procedure

In our simulation environment, the procedure of the system simulation is as follows. The primary and secondary transmitters randomly generate binary symbols which are either one or zero. Then, the primary signal is encoded by Turbo encoder and the secondary signal is encoded by Raptor encoder, respectively. The details of these two channel codes were specified previously. After that, these two signals experience the additive white Gaussian noise.

At the receiver, the SIC scheme is performed to decode the received signal. As the power of the secondary signal is stronger than the primary signal, it is easy to decode the secondary signal by Raptor decoder. Then, this successfully decoded signal is re-encoded to generate a replica of the secondary signal. An interference free of the primary signal with additive white Gaussian noise is obtained by subtracting this replica of the secondary signal from the received signal. Finally, the primary Turbo decoder decodes the primary signal.

The Monte Carlo method is used in our simulation. For each SNR point, the simulation will not stop until 100 error events occur.

3.4.3 Simulation Results

In order to compare the simulation results with the performance of single transmission, we define an RMS ratio δ which is the square root ratio of two signals'

power levels $\sqrt{P_1}$ and $\sqrt{P_2}$ as follows:

$$\delta = \sqrt{P_1}/\sqrt{P_2} \quad (3.4)$$

This ratio indicates the power relation between the two signals.

The performance of single Turbo codes transmission in terms of different power levels is first shown in Fig. 3.3 to get clues of the system performance. As we can see from the figure, the performance of the Turbo code with a 0.3 fading factor follows the same trend from 10 dB, compared to the Turbo code's with power level equalled to 1.0. This fading factor is just the attenuation of the signal power.

According to the conversion Equation 3.5 with dB converted to power gain,

$$SNR = 10^{SNR_{dB}/10} \quad (3.5)$$

if we choose $SNR_{dB} = 13dB$ for example, the SNR equals to 19.95262315. As the noise power is set to 1, this SNR is the signal power. The power of the signal with an RMS ratio 0.3 can be calculated as $0.3^2 \cdot SNR$, and therefore equals to 1.795736083. The decibels can be obtained by the reverse of the Equation 3.5, and equals to 2.54 dB. Therefore, the number of error bits based on two different received signals at 2.54 dB and 13 dB should be the same. According to the simulation results in Fig. 3.3, compared with the two signals' performance at 2.54 dB and 13 dB, respectively, the BER values are almost the same, and the gap

between these two signals is around 10.46 dB.

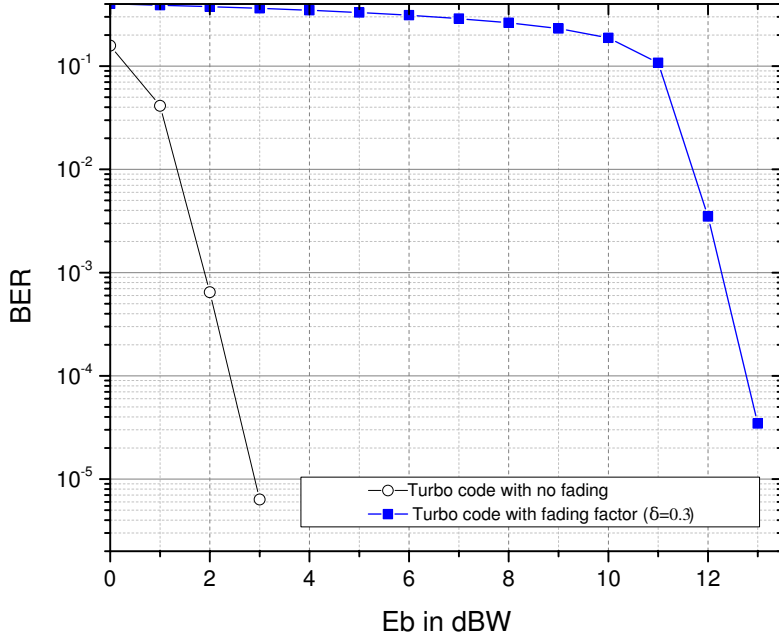


Figure 3.3: BER performance of Turbo code over AWGN channel versus normalized transmitted power

The system simulation result is shown in Fig. 3.4. We first set a fixed ratio in our simulation which $\sqrt{P_2}$ equals to 1 and $\sqrt{P_1}$ equals to 0.3. As we can see from that, the primary user's performance with Turbo codes shows exactly the same bit error rate compared to the single transmission in Fig 3.3. Therefore, the primary user transmits its own signal as though there is no interference in our system. In the meantime, a good performance of the secondary user's performance with Raptor codes is depicted in this figure. As there is no loss to the primary user's performance, the increasing system capacity deploying the SIC scheme, is shown by the secondary user's performance.

In order to compare the BER of secondary transmission to single transmission, we draw another Fig. 3.5 to show the difference. From the figure, at BER 10^{-4} , we

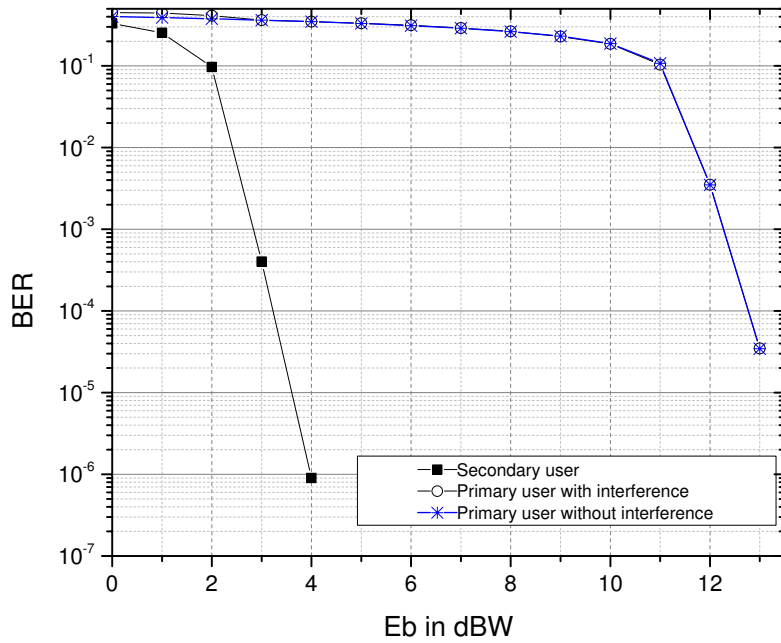


Figure 3.4: BER performance of system over AWGN channel with ratio=0.3

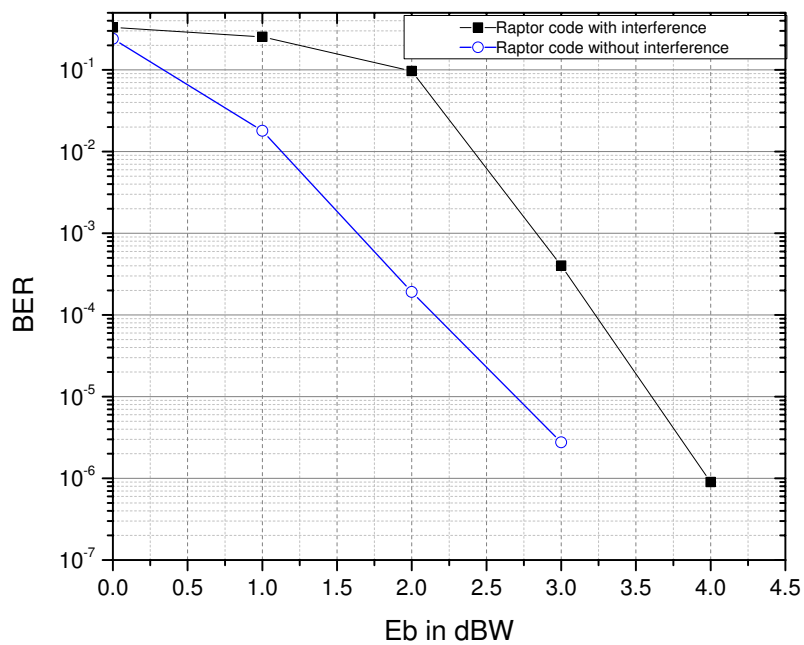


Figure 3.5: BER performance of Raptor code over AWGN channel with and without interference

can clearly see that the performance of Raptor codes with interference, as shown in Fig 3.4, is around 1.06 dB away from the single transmission of Raptor codes.

Here, the boundary of the RMS ratio δ of the two signals' power levels needs to be illustrated. When the ratio decreases, which means the power level of the primary signal is going to be smaller than the secondary's, there is still no interference to the primary transmission and the performance of the secondary transmission is getting better. Because, it is easier to decode both signals on the basis of larger power difference by using the SIC scheme as we discussed previously. On the other hand, when the ratio goes up, in other words, the power difference is minimizing, the performance of both signals are getting worse. According to the simulation results, when the ratio is around 0.64, the primary signal is clearly interfered by the secondary interfering signal at BER 10^{-2} , and therefore leads to a failure transmission to both users. With a simple CSI at the transmitter, an adaptive power control scheme can be deployed to always keep the power difference at a proper level. This scheme will be proposed in Chapter 5.

Chapter 4

Coexistence of LTE and Wi-Fi

4.1 Overview

As we know, LTE and Wi-Fi work in different bands to be isolated to each other, and therefore makes sure for a good performance for both carriers. However, there are always some channels that are unused during the transmissions in a real-world case. Besides, to ensure a satisfactory transmission, the band guards with a small bandwidth are needed. This is more important for LTE bands 7, 38, 40 and 41, which are extremely close to the existing Wi-Fi and Bluetooth bands. All these disadvantages lead to an inefficient usage of bandwidth.

Most recently a new approach and a technology are proposed to provide the probability of the coexistence of LTE and Wi-Fi. The new approach is LTE in Unlicensed Bands (LTE-U) [49]. As its name suggests, the LTE focuses on the unlicensed 5 GHz band of Wi-Fi. The technology is Download Booster which is proposed by Samsung for their mobile phone products: Galaxy S5 [50]. The

Download Booster allows a larger file (which is a single task) to be downloaded faster by deploying both LTE and Wi-Fi. The details of these two new technologies will be discussed in the following section.

Based on the background of wireless communication, the coexistence of LTE and Wi-Fi system we propose in this thesis contributes not only a proposal that allows LTE and Wi-Fi transmit in the same band simultaneously, but also a scheme which is the combination of two antennas into one. The inefficiency of wireless communication and the ability of processing only single task can be promoted by the proposal of the coexistence system. This system increases the efficiency of the bandwidth usage and handles different tasks at the same time. On the other hand, the combination of two antennas into one provides a design of hardware in mobile devices that saves space. The antenna configuration of the coexistence of LTE and Wi-Fi will be proposed in this chapter.

4.2 Feasibility of the coexistence

In Chapter 2, the solutions for the problems of the coexistence of LTE and Wi-Fi in adjacent channels have been illustrated. In this section, we will discuss the feasibility of the coexistence of LTE and Wi-Fi in the same channels.

LTE-U is proposed to provide us a new perspective to deploy LTE in the unlicensed bands with the coexistence of Wi-Fi. On the other hand, the Download Booster technology, which is proposed by Samsung, allows users to download a

large file faster than before by combining both LTE and Wi-Fi networks at the same time. All of these aspects provide us with a foundation to design a new coexistence system between LTE and Wi-Fi.

4.2.1 LTE in the unlicensed bands

In late 2013, the idea of LTE in unlicensed spectrum was proposed in a 3GPP meeting. In this meeting, the drivers, benefits, challenges and deployment for LTE in unlicensed spectrum were first discussed and suggested [51], [52], [53]. Half a year later, a 3GPP workshop on LTE in unlicensed spectrum was held in France. The coexistence considerations of LTE in unlicensed spectrum [54] and [55], the LTE carrier aggregation with unlicensed spectrum [56], and the benefits of extension LTE to unlicensed spectrum [57] were proposed and discussed.

Here, we mainly focus on the coexistence considerations of LTE in unlicensed spectrum with Wi-Fi. As suggested in these reports, there are three schemes that are proposed for LTE-U to coexist with Wi-Fi. The first scheme is a dynamic clear channel selection scheme. Based on the interference, the LTE-U dynamically selects a clear channel. The second scheme is Carrier Sensing Adaptive Transmission (CSAT) scheme for LTE-U. This scheme requests the LTE-U to sense the channel before the transmission. As we know, Carrier Sense Multiple Access/Collision Avoidance (CSMA/CA) is a protocol for carrier transmission in 802.11 networks. If LTE-U coexists with Wi-Fi in the same channel, it is very likely that Wi-Fi will always back-off. Therefore, a CSAT scheme is proposed for

a fair coexistence. Also, according to this fair coexistence purpose, a Listen Before Talk (LBT) scheme is suggested to 3GPP Release 13 for discussion.

A system performance of LTE (without any sensing schemes) and IEEE 802.11 coexisting on a shared frequency band was studied in [58]. The simulation results showed that the Wireless Local Area Network (WLAN) was interfered with by the co-existence with LTE but the severity of the interference could be controlled by a muting pattern for LTE. [59] evaluated the performance of LTE and Wi-Fi coexistence in unlicensed bands. Simulation results showed that the Wi-Fi channel was silent more than 96% of the time, in terms of the LTE interference. Therefore, the throughput of Wi-Fi decreased from 30% to $\approx 0\%$. According to all the simulation results, we can conclude that in such a coexistence system, LTE is slightly affected by Wi-Fi, but Wi-Fi is severely interfered with LTE.

To the contrary, by applying the schemes for LTE-U we discussed above, [57], [60], and [61] showed a good performance of the coexistence system. In [57], a 3.1 times gain could be obtained by replacing one Wi-Fi node by LTE-U. The performance of LTE-WLAN coexistence by applying LBT scheme is much better than WLAN-WLAN coexistence in [60]. In [61], 8 pairs of APs and Wi-Fi terminals were configured. An increase from 3.3 Mbps to 6.7 Mbps can be achieved by adding a 9th LTE-U equipment instead of a Wi-Fi terminal. In the meantime, the other 8 pairs almost maintain the same performance. Therefore, we can conclude that LTE-U is a better neighbor to Wi-Fi than Wi-Fi itself.

4.2.2 Download Booster

It is usually impossible that a UE connects both LTE and Wi-Fi at the same time to access the internet. Recently, however, the new Galaxy S5 adopted a new technology named Download Booster, which doubles the download speed by connecting both LTE and Wi-Fi. This is not only an improvement on the hardware design, but also a software enhancement.

This technology can be illustrated as follows. When a user enables this Download Booster function to download a large file, any data that is set to download via Wi-Fi only will also be downloaded via LTE network. This file will be split up into several packets as tasks. Then, these tasks are distributed to the dual IP stack connections over both LTE and Wi-Fi. Finally, the file is reassembled from these download packets. The experiments [62] and [63] showed that the download speed is approximately 80 ~ 90% of the combined network speed of LTE and Wi-Fi, as Samsung claimed.

4.2.3 Feasibility

We propose a coexistence of LTE and Wi-Fi system in this thesis. The feasibility of the hardware designs needs to be verified. According to the technologies we discussed in the chapter, the theoretical foundations and practical conditions are established. The concept of the LTE-U provides us the possibility of the coexistence transmissions under the same unlicensed bands. The Download Booster function allows the LTE and Wi-Fi transmit simultaneously by combining the hardware

and software coexistence design together. These all make the new coexistence system feasible, not only for a theoretical model but also for implementation.

4.3 Antenna design of the coexistence of LTE and Wi-Fi

In this section, the hardware design is discussed. As is well-known, the design of antenna locations in a mobile device plays a very important role in the electronic industry. A severe interference will be caused if the antenna dimensions and separation distances are not designed very well. Meanwhile, as the space of mobile devices is usually very limited, the more antennas are needed, the more complexity of a design is required to be considered. Therefore, a design of one antenna

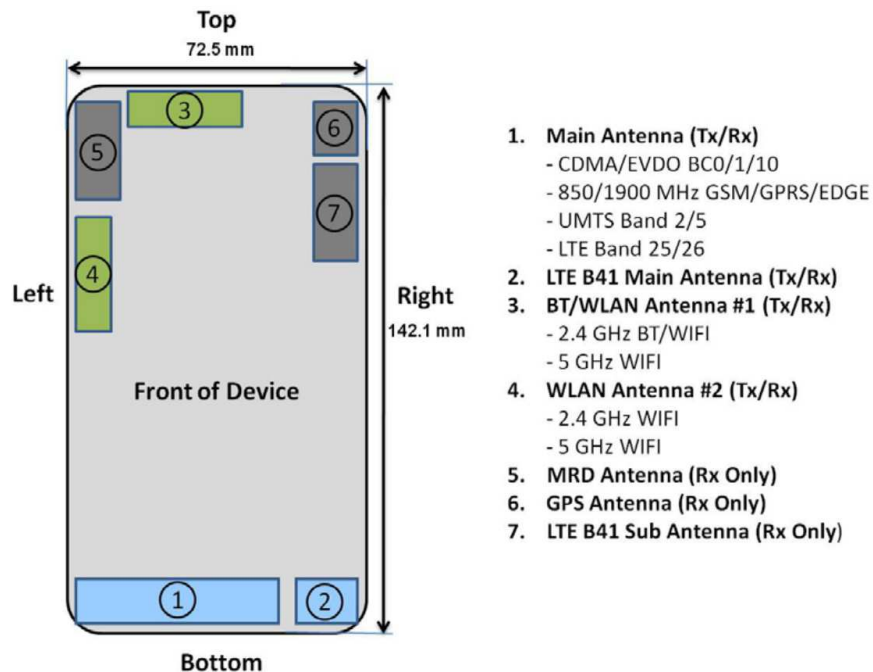


Figure 4.1: Antenna Locations of Galaxy S5 [3]

(which is integrated by two or more antennas) allowing both LTE and Wi-Fi

transmissions, will be a huge influence on the system design.

Fig. 4.1 [3] shows the antenna locations of the Samsung Galaxy S5. There are 7 antennas integrated into this device. As we can see from the figure, two 3G/LTE antennas are isolated from the other antennas, especially the two Wi-Fi antennas. Because some bands of 3G/LTE are so close to the Wi-Fi bands, and they need some distance to make sure there is no interference.

As proposed in our thesis, the coexistence system allows LTE and Wi-Fi to transmit their own signals in the bands simultaneously. Therefore, a new antenna integration design is proposed, compared to the existing antenna configuration.

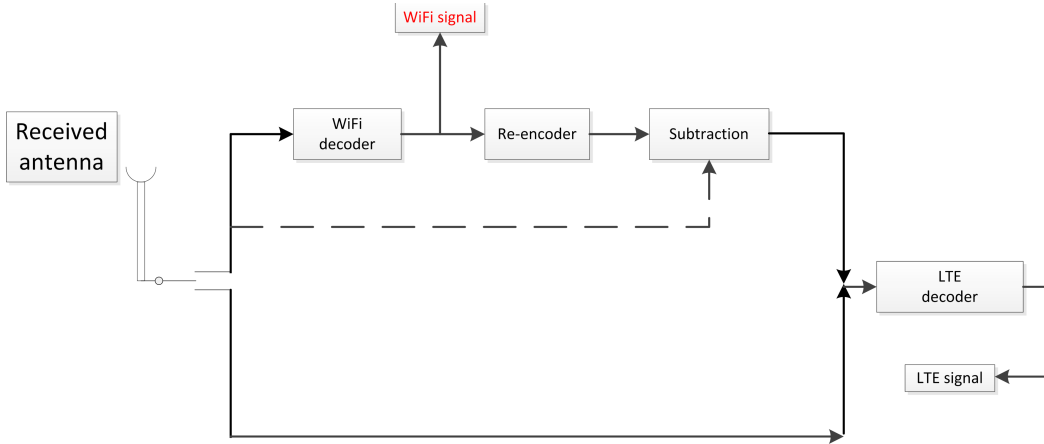


Figure 4.2: The new design of antenna integration

This new design is illustrated in Fig. 4.2. The received antenna represents an integration of LTE and Wi-Fi antennas. There is a switch after the antenna. When the received signal is only transmitted from LTE, the switch connects to the down link and sends the signal directly to the LTE decoder. When the received signal is transmitted from both LTE and Wi-Fi, the switch connects to the up link

and follows the SIC scheme. The Wi-Fi signal can be obtained from the Wi-Fi decoder. The details of SIC scheme in this coexistence of LTE and Wi-Fi will be illustrated in Chapter 5.

This new design combines two antennas into one. As a result, we save some space in the mobile devices. In the meantime, as LTE and Wi-Fi work in the same bands, there is no more interference needed to be considered.

Chapter 5

System Model: Turbo and Raptor Coded SIC with Channel State Information

5.1 Overview

In this chapter, a system enabling the coexistence between LTE and Wi-Fi is proposed. A Base Station (BS) and an Access Point (AP) are the main transmitters in our system, the receiver is a UE deploying an effective SIC receiver. The Rayleigh fading channel is considered as it is the model usually used for wireless transmission situation.

The Rayleigh fading channel is a suitable model to represent the real world wireless channel and it is also easy to calculate and quantize in the research en-

vironment. In Chapter 3, we achieved some results for AWGN channel and now we move on to the Rayleigh fading channel to analyze and get simulation results according to the LTE and Wi-Fi wireless communication environment.

From another point of view, AP to UE as an interfering channel of Wi-Fi link is proposed to add into the existing LTE main link. As we proposed in Chapter 3, the overall throughput increases by sharing the same channel by two users where the successive interference cancellation scheme is employed. The LTE link, which cohabits with the Wi-Fi interfering channel, transmits signals as though there is no interference. That is by using SCI scheme, the effect of Wi-Fi interference is completely removed.

The performance of SIC scheme is best when the power difference between the two sources is considerable. This fact makes the coexistence between LTE and Wi-Fi a good application. Because the latter works in indoor environments leading to a high level power and the former at low power level as it experiences long distance path loss and Rayleigh fading. However, when another user is located far away from the Wi-Fi transmitter and therefore the received power of Wi-Fi signal is a little higher or almost the same compared to the LTE signal, this SIC scheme cannot work well to decode both signals correctly. Therefore, a secure distance around the Wi-Fi transmitter needs to be guaranteed. The RMS ratio boundary has been achieved in Chapter 3. According to this ratio and based on the the received signal power of LTE, we can obtain a desired range of the Wi-Fi power in terms of the distance. A desired performance can be achieved based on the power

and the distance.

5.2 System Model

As we discussed the system model over AWGN channel in Chapter 3, here we propose another system model where the fading is considered and it is phase-coherent, which means the phase of the channel fading is assumed to be known but we need to estimate the amplitude. Consider both the primary transmitter like LTE and the secondary transmitter like Wi-Fi sending data streams to the same destination over a fading channel. The received signal can be expressed as follows:

$$y = h_1 \cdot \sqrt{P_1} \cdot x_1 + h_2 \cdot \sqrt{P_2} \cdot x_2 + z \quad (5.1)$$

where h_1 and h_2 are the channel fading coefficients, P_1 and P_2 are the energy per bit for the main source and interfering source, respectively.

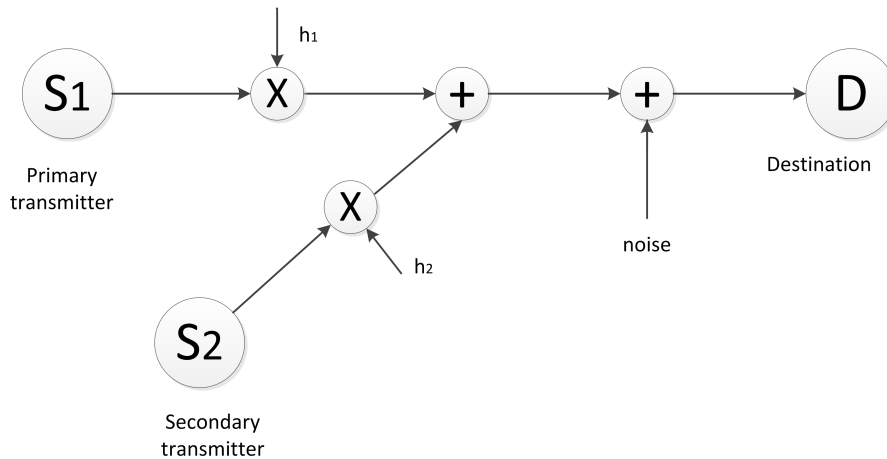


Figure 5.1: System model over fading channel

The system block diagram is shown in Fig. 5.1. The channel fading coefficient introduces a huge effect to the existing signals and usually causes some error frames. In such circumstances, the error frames need to be dropped and a retransmission request will be sent from the receiver to the transmitter. The estimation of the channel state information is introduced to solve this problem and we will propose a scheme later.

5.3 Proposed Scheme

Here, we investigate two situations. In the first case: h_1 and h_2 vary following a memory size which is usually shorter than one block. This method is used in [64] to evaluate the block fading channel and it is an important way to simulate the wireless channel. A variety of practical communication systems, such as the Orthogonal Frequency Division Multiplexing (OFDM) and Time-Division Multiple Access (TDMA) systems are illustrated by this model [64]. In the second case: the channel fading coefficients change in each block. Under such situations, the channel fading coefficient doesn't vary in one block. It is usually recommended to drop the whole block if a Cyclic Redundancy Check (CRC) indicates an error frame and an ARQ method is needed. Along with the two cases, an adaptive power control scheme will also be proposed.

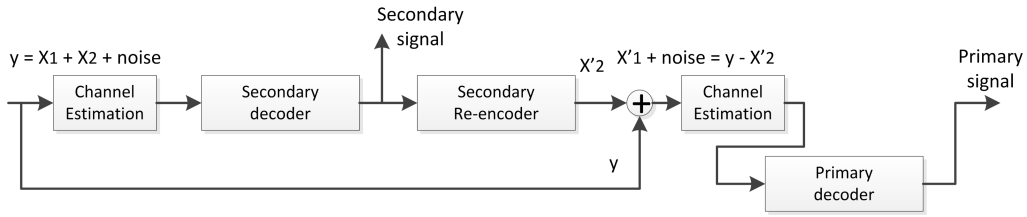


Figure 5.2: Successive interference cancellation scheme with channel estimation

5.3.1 System over block fading channel with small memory size

Fig. 5.2 shows the system model. Before the received signal goes to both primary and secondary decoders, we add an estimation process to estimate the channel state information. The channel state information at the receiver does a favor for both decoders. As a result, both the Turbo decoder and the Raptor decoder will decode more accurately and therefore improve the performance according to the more precise information and diversity from the channel.

The joint channel estimation scheme draws a lot of attention among researchers and scholars. The insertion of pilot symbols which assists the channel estimation and iterative decoding for Turbo codes over the fading channel is proposed in [65]. The Maximum Likelihood (ML) techniques and MAP techniques are used in [64] to estimate the CSI based on LDPC codes. The Minimum Mean-Square-Error (MMSE) estimate of the channel is adopted for estimating CSI according to Raptor codes in [66]. These schemes are based on iterative decoding schemes. After each iteration, the decoder generates a new channel estimate through passing either the hard decisions or the soft decisions back to the estimator and updates the LLR.

In our proposed scheme, we adopt a new channel approximation scheme which is proposed in [13]. The pilot symbols are no longer needed and the decoding process does not require to update the estimation value for each iteration. The estimation value is defined as follows:

$$\hat{h} = \frac{\bar{y}}{\sqrt{P}} \quad (5.2)$$

where \hat{h} is an estimate of the channel state information, P is the signal energy per bit, and \bar{y} is the square root of the average received signal power where the average is over the channel memory size. This can be expressed as:

$$\bar{y}^2 = \frac{1}{n} \sum_{i=1}^n y_i^2 \quad (5.3)$$

where n is the block memory size. The estimation is perfect when the Gaussian noise of the received signal y is negligible.

Unlike the ML and MAP estimation schemes, the estimation value of this scheme is obtained before an iterative decoding process and used in the decoder. The performance is a little worse than the MAP estimation and the results have been shown in [13]. According to the simplicity and the short latency of this process, this new scheme is a practical method to estimate the channel in some specific environment. We also predict that the performance of this scheme depends on the channel memory size, which the gap of the BER performance between the joint estimation decoding and the perfect channel knowledge decoding shrinks when the

memory size increases. The simulation results shown later verifies the prediction.

5.3.2 System over block fading channel with large memory size

As opposed to the fading channel with a small memory size, the channel fading coefficients changing at each block is totally another situation and the channel is usually called slow block fading channel. Under such conditions, the channel fading coefficient remains constant over one block. If an error frame occurs in the fading channel, it is required to drop the whole block. The system block diagram of the second case is depicted in Fig. 4.3.

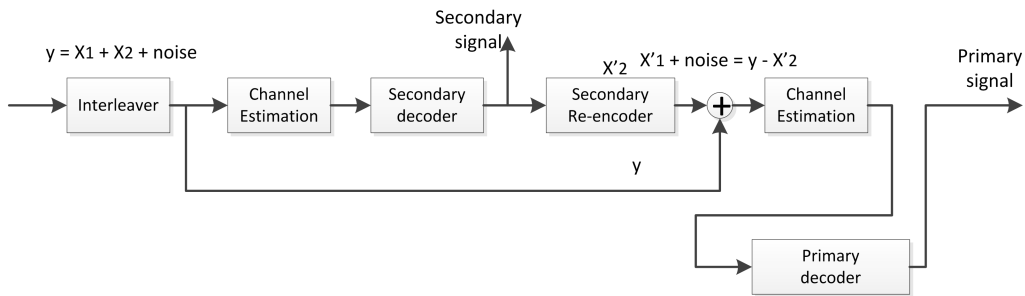


Figure 5.3: Successive interference cancellation scheme with an interleaver

Slow block fading channels, such as this always lead to severely undesired transmission and it is not easy to get rid of the disadvantage. The reason is that the channel estimation information is useless at the receiver to perform some jointly channel estimation decoding scheme to achieve a better performance because there is usually not much diversity in one block in terms of this fading channel. As a result, the decoder of channel codes, such as Turbo codes and Raptor codes, have no room to increase the quality of transmission.

In order to overcome the difficulties caused by a slow fading channel, an interleaver is introduced. We have already been familiarized with the interleaver function which was discussed in Chapter 2. Different from the interleaver used in Turbo codes, here we propose an ordered interleaver. For example, suppose we have 100 stand-by blocks needed to be sent at the transmitter and 2000 bits per block. At the transmitter, the interleaver takes the first 20 bits from every block and assembles them into a new block named new block no.1. This block can be sent immediately. In the meantime, the new block no.2 is being assembled by the interleaver in order, which means the second 20 bits of every block are taken out. By performing this process sequentially, the new 100 blocks are constructed. At the receiver, on the other hand, the deinterleaver reconstructs all the received bits to the original blocks. As a result, each 20 bits in the reconstructed block experience a different fading, and therefore introduce more diversity in one block. The interleaver size is adjustable and different number of blocks can be chosen. This method can be imagined as a solution which converts the slow block fading channel to a block fading channel with a small memory size. Therefore, the performance can be inferred to be the same. However, there is still a little difference and the simulation results will be shown subsequently.

5.3.3 Adaptive power control scheme

The systems with no CSI and with the CSI at the receiver were discussed before. In Chapter 3, the boundary of the RMS ratio of the two signals' power levels has been illustrated. In order to guarantee the quality of both transmissions, this

ratio should be limited within a scope. From another point of view, it is better that the power of the secondary transmitter be adjusted to adapt with different channel conditions especially with interference. Therefore, an adaptive power control scheme with the CSI at the transmitter is proposed. Figure. 4.4 shows the procedure of this scheme.

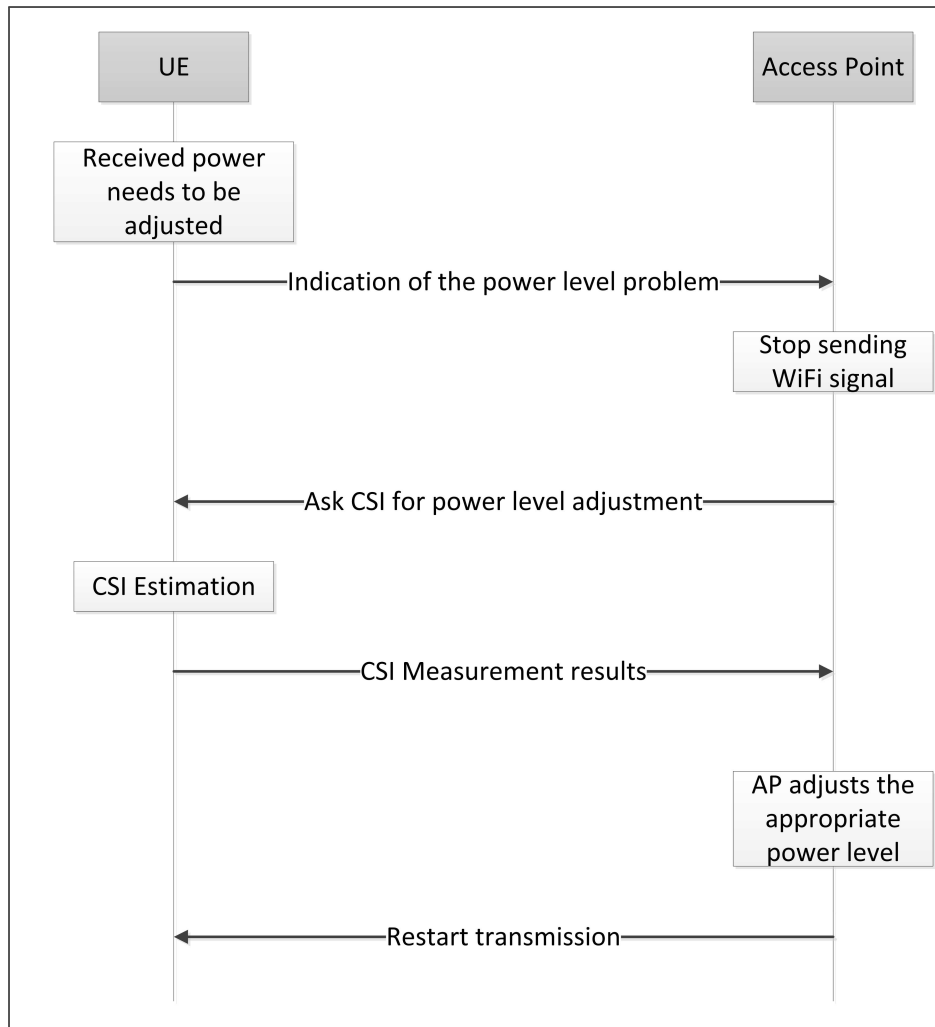


Figure 5.4: Adaptive power control scheme

The scheme can be explained as follows:

- 1: The UE receives both signals and determines whether it could decode the Wi-Fi signal correctly.

- 2: If an error occurs, a message will be sent from the UE to indicate the power level problem to the Wi-Fi AP.
- 3: Then, the Wi-Fi AP stops sending the Wi-Fi signal to avoid interference. Ask the CSI of the channel.
- 4: The UE estimates the CSI and the LTE signal power.
- 5: A feedback is sent to the Wi-Fi AP.
- 6: A proper power level as desired is adjusted according to the CSI and the estimated LTE signal power. Then, restart to send the Wi-Fi signal.

5.4 Simulation Results

In our simulations, the configurations of both Turbo codes and Raptor codes are the same as we illustrated in Chapter 3. Here, the measurements of the received power for both LTE and Wi-Fi signals have been done in the lab of Concordia University. The Wi-Fi provider is Concordia University and the LTE carrier is Fido. We measured 50 times in different hours of a day. The average power of Wi-Fi signal is around -65 dBm and the average power of LTE signal is around -95 dBm. This indicates that the Wi-Fi signal is 1000 times stronger than the LTE signal. Therefore, a parameter $1/\sqrt{1000}$ which is around 0.0316 can be obtained if we use the RMS ratio of the two users to represent. In our simulation, this ratio is chosen to be 0.3. There are two reasons why we choose this ratio value. The first reason is 0.3 is ten times worse than the measurement value, this means we choose a very worse case in our simulation. If the simulation reveals a good performance,

we can reasonably infer that a smaller ratio could achieve a better result and we will present another simulation result based on 0.2 ratio to show the trend. The other reason is that it is convenient to compare with the simulation results over the AWGN channel which we have already had in Chapter 3.

We consider a Rayleigh block fading channel with a memory size, where the fading coefficient is constant over the transmission of the memory size. This memory size is chosen from 10 to the whole block size value. On the base of different memory sizes, different schemes, such as the estimation scheme and the interleaver method are applied to achieve a good performance.

We first investigate the scenario which the CSI is available at the receiver. In our system, Wi-Fi works in the indoor environment, we can easily get the channel information before the whole system runs. Therefore, we assume a perfect CSI of the Wi-Fi channel is available at the receiver. For the LTE transmission, the new CSI estimation scheme we discussed previously is adopted, and the performance is compared to the results with no CSI and with perfect CSI at the receiver. Then, the scenario with CSI available at the transmitter is simulated. A desired transmit power of Wi-Fi transmission is chosen for simulation.

5.4.1 Simulation Results over block fading channel with a small memory size

The simulation results for the coexistence of LTE and Wi-Fi over a block fading channel with a 10 memory size and a 20 memory size are shown in Figures 5.5

and 5.6, respectively. The RMS ratio of the two signals' power levels is chosen to be 0.3. The estimated CSI of LTE channel is obtained before decoding at the receiver by using the new estimation scheme. The perfect CSI of Wi-Fi channel is available at the receiver. Compared with these two figures, the performance with a 10 memory size is better than the 20 memory size. The reason is the decoder has more diversity in one block with small memory size than the large size, and therefore leads to decode more correctly and precisely.

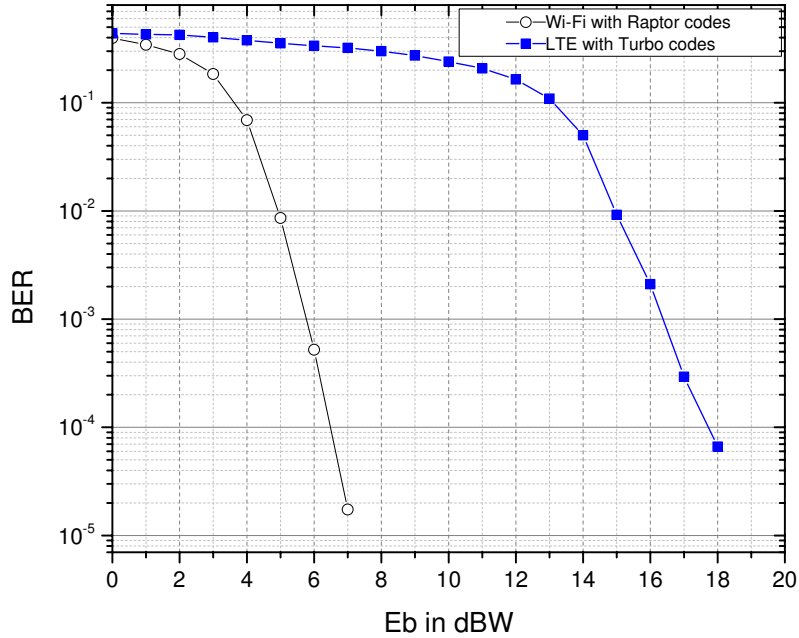


Figure 5.5: BER performance of the coexisting LTE and Wi-Fi transmissions over block fading channel with memory size=10, ratio=0.3

In order to compare the LTE performance, the simulation results of the single LTE transmission with Turbo codes in terms of different channel state information are shown in Fig. 5.7. As we can see from the figure, the middle curve represents the BER performance of the single LTE transmission with estimated CSI at the receiver. Compared to Fig. 5.5, the LTE transmission in the coexistence system

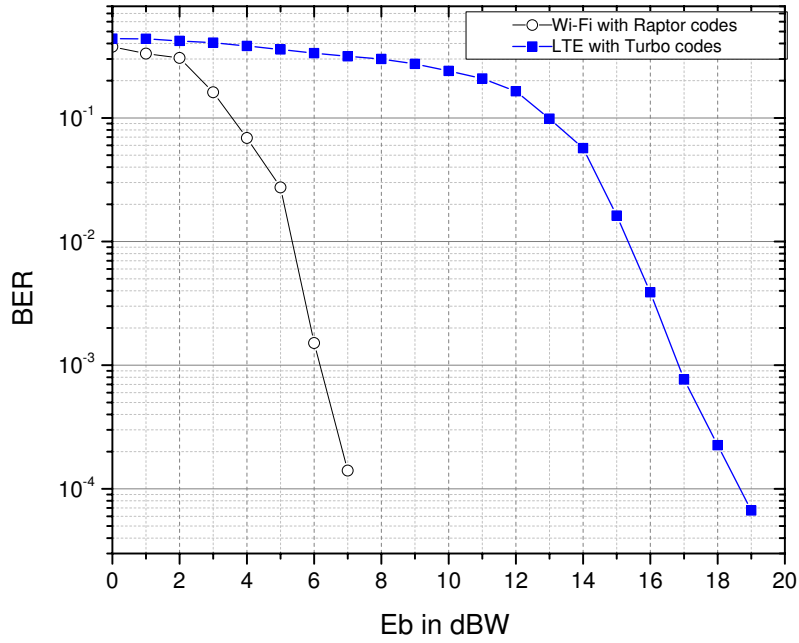


Figure 5.6: BER performance of the coexisting LTE and Wi-Fi transmissions over block fading channel with memory size=20, ratio=0.3

shows the same BER performance as it is shown in Fig. 5.7. Therefore, it can be concluded that there is no interference introduced to the existing LTE link when we add another Wi-Fi link.

Consider the BER performance of Wi-Fi transmission in the coexistence system. According to the simulation results that we achieved in Chapter 3, this performance is a little worse than single Wi-Fi transmission. If we increase the power difference which the power of Wi-Fi is much stronger than the LTE, a better performance will be achieved and finally leads to two transmissions over a fading channel with no interference to each other at some point. Regardless, without introducing any interference to the existing link, this increased capacity is incredible.

As shown in Fig. 5.7, at BER 10^{-4} , there are a 0.70 dB gap between the performance of perfect CSI and estimated CSI, and a 0.71 dB gap between the performance with no CSI and with estimated CSI, respectively.

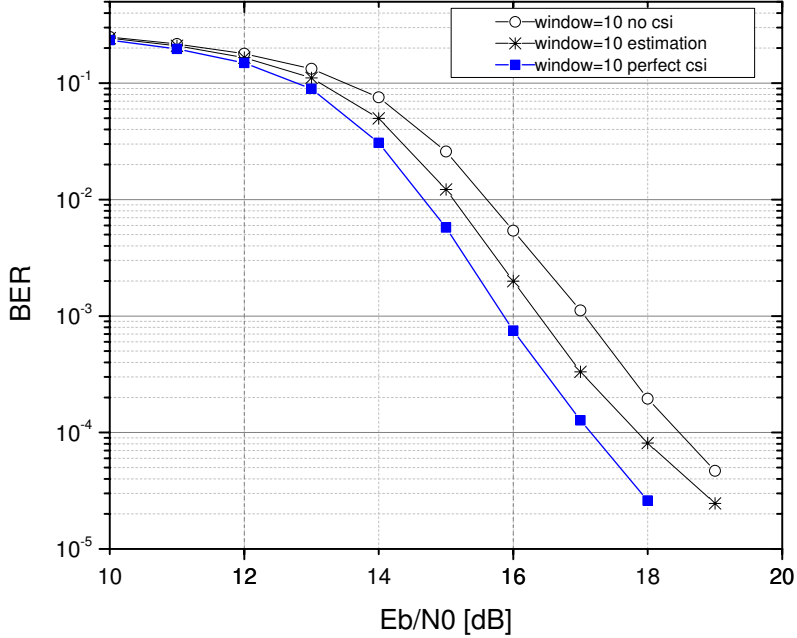


Figure 5.7: BER performance of single LTE transmission over block fading channel with memory size=10, ratio=0.3

The performance of the new estimation scheme can be illustrated under different memory size conditions. In comparison with the simulation results shown in Fig. 5.7, the new estimation scheme with a larger 20 memory size achieves a better performance in Fig. 5.8. At BER 10^{-4} , the gap between the performance of perfect CSI and estimated CSI is just around 0.4 dB. By increasing the memory size from 10 to 20, we have a 0.3 dB gain. It is easy to understand this result, because the estimation value of the channel state information \hat{h} is based on the average

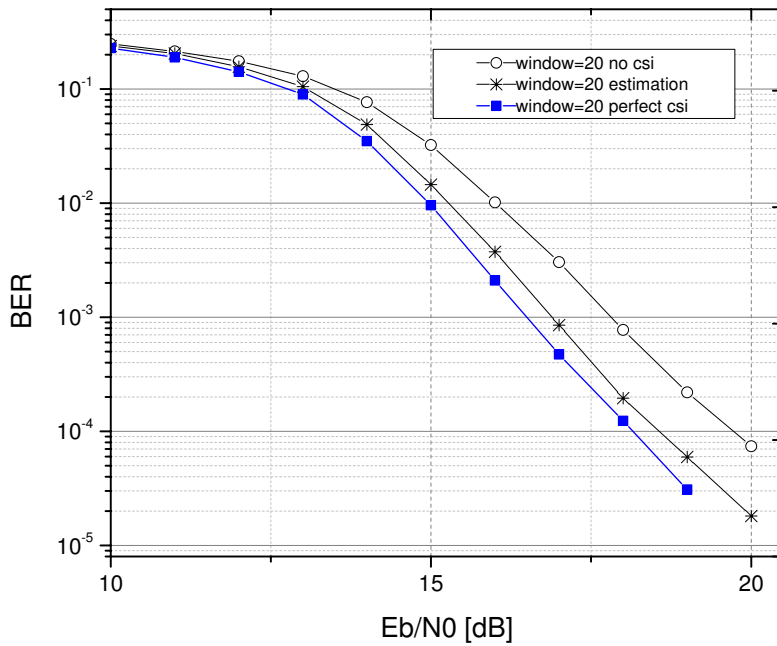


Figure 5.8: BER performance of single LTE transmission over block fading channel with memory size=20, fading factor=0.3

received signal power in a memory size. When the memory size increases, the average received signal power is more accurate. Therefore, it can be summarized that the performance of this new estimation scheme depends on the memory size of a fading channel, and a better performance can be achieved with a larger memory size.

5.4.2 Simulation Results over block fading channel with a large memory size

The simulation results for the coexistence of LTE and Wi-Fi over a block fading channel with a block memory size by using an interleaver at both the transmitter and receiver, are shown in Figures 5.10 and 5.11. The interleaver can adjust its

order based on different requirements. We simulate two cases according to the order of the interleaver. The first case is that each time only one bit from every stand-by original block is taken out to assemble a new block. Then, these new blocks will be sent to the receiver over a slow block fading channel. At the receiver, the original blocks will be reconstructed from the received blocks and sent to the decoder. The second case is 10 bits are collected from each original block to form a new block.

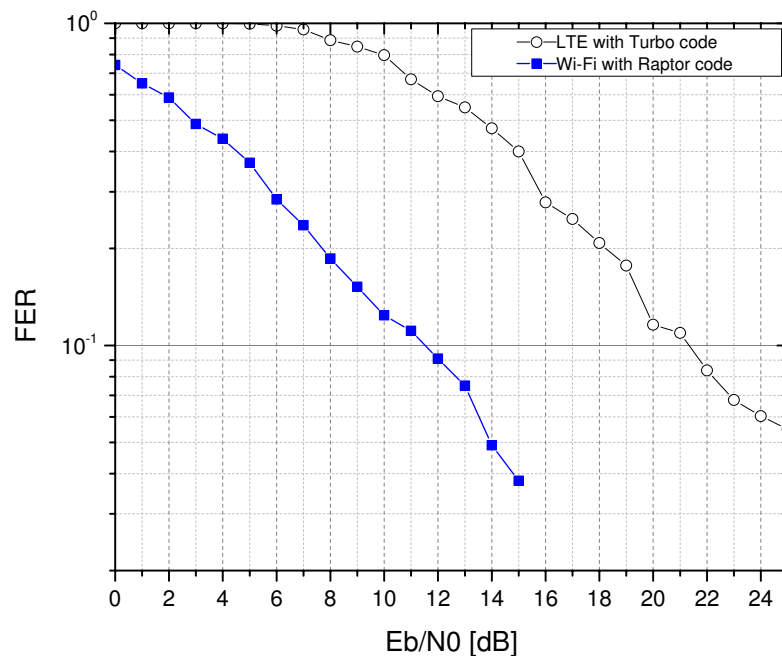


Figure 5.9: FER performance of the coexisting LTE and Wi-Fi transmissions over slow block fading channel with no interleaver

As we know, a slow block fading channel, which the channel fading coefficient remains constant in one block, can lead an error frame if the channel fading coefficient is really small. The whole block needs to drop under such a condition. As a result, the BER performance of a system is really undesired and it is usually to use a Frame Error Rate (FER) to illustrate the performance of a system. Figures

5.9 shows the FER performance of the coexisting LTE and Wi-Fi transmissions over slow block fading channel. As we can see from the figure, both transmissions cannot achieve a good performance. This is the reason we propose an ordered interleaver in our system.

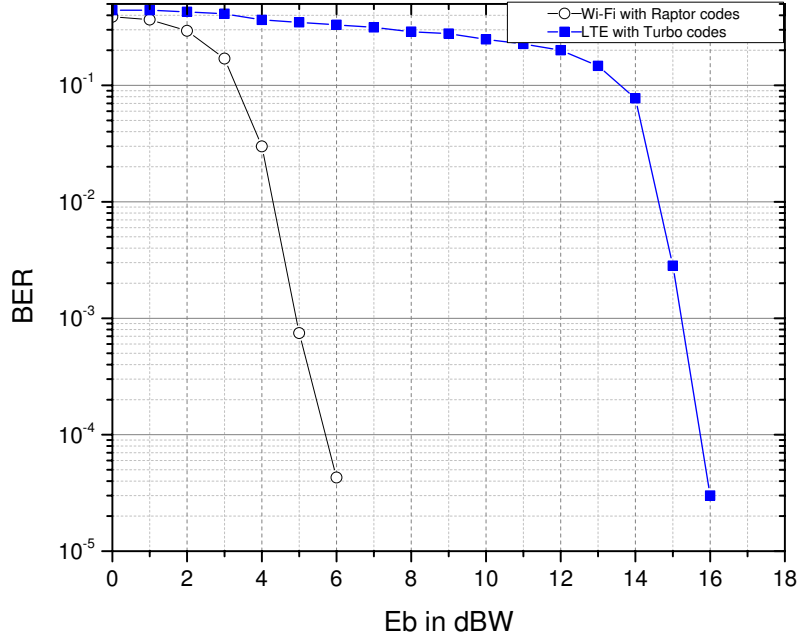


Figure 5.10: BER performance of the coexisting LTE and Wi-Fi transmissions over slow block fading channel with interleaver size=1

As we can see from the figures 5.10 and 5.11, the simulation results show a difference according to the different interleaver sizes. At BER 10^{-4} , the BER performance of Wi-Fi link with an 1-bit interleaver is around 0.4 dB better than the 10-bits', and the BER performance of LTE link with an 1-bit interleaver is around 1.3 dB better than the 10-bits'.

Compare to the Fig. 5.5 which illustrated the BER performance of the co-existence of LTE and Wi-Fi over block fading channel with a 10 memory size. Although the signals of the system with a 10-bits interleaver can be assumed to

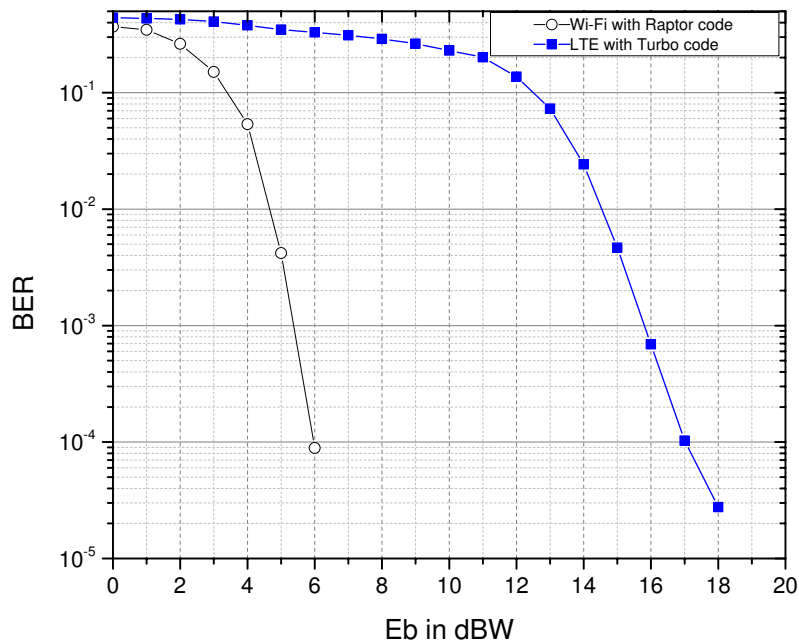


Figure 5.11: BER performance of the coexisting LTE and Wi-Fi transmissions over slow block fading channel with interleaver size=10

experience the same fading channel, the Fig. 5.11 still shows a better performance. The reason is that the estimated CSI of the system with a 10-bits interleaver is more accurate in terms of the number of the whole block size.

However, there is a disadvantage of this method. Although the total processing time is just a slight longer because of the process of the interleaver, in order to reconstruct the original blocks at the receiver, each block needs to wait until the last block is received. This will lead a delay to each block, and therefore influences the system. There is a trade-off between the choice of the number of stand-by blocks and the system performance. If we choose a larger number of blocks, the performance will be better, but the waiting time is relatively longer.

5.4.3 Simulation Results with adaptive power control scheme

By using the adaptive power control scheme, a transmitted power of the Wi-Fi transmission can be adjusted to a desired level. In Fig. 5.12, the simulation results of the coexistence of LTE and Wi-Fi over block fading channel with a 10 memory size and a 0.2 ratio are shown.

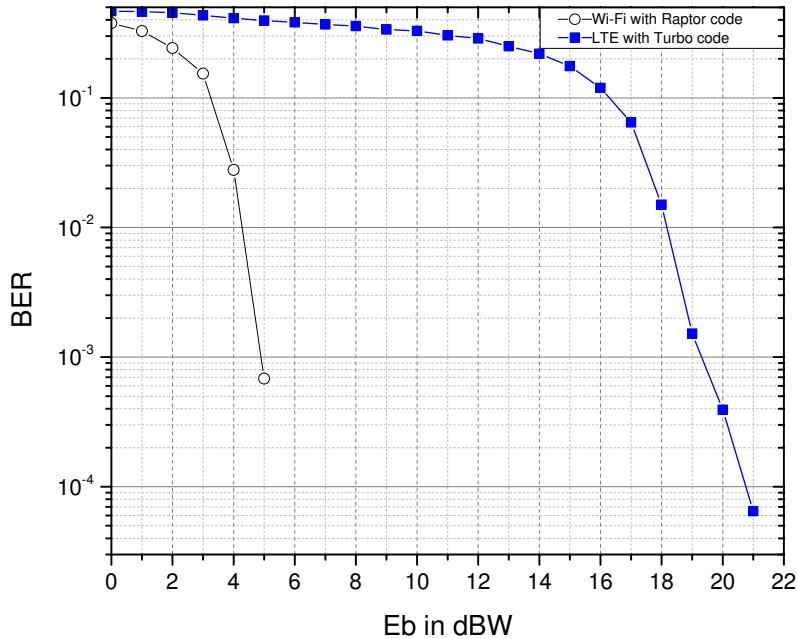


Figure 5.12: BER performance of the coexisting LTE and Wi-Fi transmissions over block fading channel with memory size=10 and ratio=0.2

As we can see from the figure, the performance of Wi-Fi transmission with a 0.2 ratio is 1.2 dB better than the performance with a 0.3. Therefore, according to the measurement we have done previously, we will achieve a simulation result of Wi-Fi transmission with the 0.0316 ratio, as though there is no interference to this link.

Chapter 6

Concluding Remarks

6.1 Conclusion

In this thesis, we investigated a coexistence of LTE and Wi-Fi. Multiple schemes in terms of different channel conditions and scenarios, as well as a new design of antenna configuration, were proposed.

In Chapter 3, coexistence of a primary user and a secondary user under AWGN channel with no CSI was proposed. The Turbo codes (which is standardized in 3GPP) were applied as the channel codes for the primary user and could be replaced by LDPC codes as suggested for DVB transmissions. Meanwhile, the secondary user adopted the Raptor codes to transmit its signal. The Raptor codes can adjust the code rate in terms of different channel conditions and interference, and do not introduce a large delay. Therefore, the Raptor codes are suitable for an adaptive transmission system with interference.

An interfering channel from the secondary user to destination is proposed to add into the existing main channel. We assume that there is a power level difference between two users, where the power of the secondary user is higher than the primary user's. Therefore, the SIC scheme is applied in the proposed system to guarantee the performance of both transmissions. The interfering signal, which is from the secondary user, is decoded first, and then the main source signal is decoded.

According to the simulation results of different channel codes we have done in Chapter 2, the simulation parameters of the coexistence system were properly chosen. The simulation results showed that the performance of the primary user with interference is the same as the single transmission performance. That means the effect of secondary user interference is completely removed by using the SIC scheme. Therefore, the increasing system capacity is shown by the performance of the secondary user.

In Chapter 4, we proposed a new antenna integration design where an antenna is integrated by two antennas. We reviewed the two most recent approaches: the LTE-U and the Download Booster function. LTE-U is a coexistence of LTE and Wi-Fi which transmit signals in the same unlicensed bands using some back-off schemes, and Download Booster function is a data download method that works by connecting both LTE and Wi-Fi under different bands simultaneously. The feasibility of the new design, therefore, was demonstrated. The antenna design of the coexistence of LTE and Wi-Fi was proposed. As a result, the space of mobile

devices will be saved.

In Chapter 5, a coexistence between LTE and Wi-Fi with CSI under Rayleigh fading channel was proposed. The SIC scheme was also applied. Two schemes were proposed based on different channel conditions. The first scheme is based on a block fading channel with a small memory size. A new channel estimation scheme is adopted for the CSI estimation at the receiver. The second scheme suggests to deploy an interleaver to overcome the difficulties caused by a block fading channel with a large memory size. The interleaver size can be adjusted to adapt the channel conditions.

An adaptive power control scheme was proposed. By having the CSI at the Wi-Fi transmitter, the transmitted power can be adjusted to a desired power level. This scheme guarantees a relatively good power difference level, and leads to a good performance for both LTE and Wi-Fi.

According to the simulation results, although we added a Wi-Fi interference transmission into the existing LTE transmission, the performance of LTE transmission is the same as the single LTE transmission's performance. The new estimation scheme showed a better performance when the memory size was getting larger. On the other hand, a good performance was achieved by applying the scheme with an interleaver, though this would introduce a delay. The adaptive power control scheme has a great result when the transmitted power of Wi-Fi signal is adjusted.

6.2 Future Work

There is some work that needs to be done to improve and perfect the systems, based on the models we have proposed and results we had, respectively.

In the SIC scheme, a optimum value of the power level difference between two users can be pursued. This means the maximum capacity of the system can be achieved by adjusting this value perfectly.

Furthermore, an adaptive transmission scheme, in terms of not only the power control but also a Look-Up Table (LUT), can be improved. This table contains the parameters of Raptor codes which are adopted by the secondary user. As the Raptor codes add one bit for each transmission until the codeword is decoded correctly. This will introduce a relatively large delay in the channel condition which is really undesired. Therefore, if a LUT contains the parameters, such as the SNR, code rate, block size, number of iterations, and the modulation scheme, vs. the BER or capacity rate, it will do a favor for the transmissions.

The brief procedure of this adaptive scheme can be described as follows. According to the BER performance of the secondary user, an effective SNR (which is the SINR at the receiver) can be calculated. The transmitter will check the LUT to locate the value based on the BER and the effective SNR from the receiver. Then, an adjustment will be made in terms of a desired performance. It could be a decision of how many extra bits should be sent all at once, or a transmitted power adjustment, or maybe a combination of several parameters.

Besides, the phase of the Rayleigh fading channel can be considered. Not only a power level difference can be distinguished as we discussed in this thesis, but also we can utilize a different phase angle to decode both signals correctly.

Moreover, a cooperative system which adds a relay between source and destination can be developed. By having more diversity, we can improve the system performance. The power allocation between sources and relay can be a task to deal with.

Bibliography

- [1] 3GPP. Ts 36.201 v12.1.0: LTE physical layer - general description (release 12), December 2014.
- [2] 3GPP. Tr 36.816 v11.2.0: Study on signalling and procedure for interference avoidance for in-device coexistence (release 11), December 2011.
- [3] PCTEST Engineering Laboratory. SAR EVALUATION REPORT for FCC. Certificaiton, PCTEST Engineering Laboratory, Inc, PCTEST Lab, Columbia, MD, USA, Feb, 03-17 2014.
- [4] Zhenping Hu, Riikka Susitaival, Zhuo Chen, I-Kang Fu, Pranav Dayal, and Sudhir Kumar Baghel. Interference avoidance for in-device coexistence in 3GPP LTE-advanced: Challenges and solutions. *Communications Magazine, IEEE*, 50(11):60–67, 2012.
- [5] M Reza Soleymani, Yingzi Gao, et al. *Turbo coding for satellite and wireless communications*. Springer Science & Business Media, 2002.
- [6] Michael Luby. LT codes. In *2013 IEEE 54th Annual Symposium on Foundations of Computer Science*, pages 271–271. IEEE Computer Society, 2002.

- [7] Amin Shokrollahi. Raptor codes. *Information Theory, IEEE Transactions on*, 52(6):2551–2567, 2006.
- [8] C.E. Shannon. A mathematical theory of communication. *Bell System Technical Journal*, The, 27(3):379–423, July 1948.
- [9] Sofia Martinez Lopez, Fabian Diehm, Raphael Visoz, and Baozhu Ning. Measurement and prediction of Turbo-SIC receiver performance for LTE. In *VTC Fall*, pages 1–5, 2012.
- [10] Zhiyuan Wu and Xiaofeng Wang. A new turbo multi-user receiver with recursive SIC-MMSE detection. In *Wireless Communications and Networking Conference, 2007. WCNC 2007. IEEE*, pages 922–926. IEEE, 2007.
- [11] Maria Samokhina, Kirill Moklyuk, Sunghyun Choi, and Jun Heo. Raptor code-based video multicast over IEEE 802.11 WLAN. *IEEE APWCS*, 2008.
- [12] Hsin-Ta Chiao, Shih-Ying Chang, Kuan-Ming Li, Yi-Ting Kuo, and Ming-Chien Tseng. Wifi multicast streaming using AL-FEC inside the trains of high-speed rails. In *Broadband Multimedia Systems and Broadcasting (BMSB), 2012 IEEE International Symposium on*, pages 1–6. IEEE, 2012.
- [13] Boulos Wadiah Khoueiry and M Reza Soleymani. Joint channel estimation and raptor decoding over fading channel. In *Communications (QBSC), 2014 27th Biennial Symposium on*, pages 168–172. IEEE, 2014.

- [14] Omid Etesami and Amin Shokrollahi. Raptor codes on binary memoryless symmetric channels. *Information Theory, IEEE Transactions on*, 52(5):2033–2051, 2006.
- [15] Theodore S Rappaport et al. *Wireless communications: principles and practice*, volume 2. 1996.
- [16] C. Berrou, A. Glavieux, and P. Thitimajshima. Near shannon limit error-correcting coding and decoding: Turbo-codes. 1. In *Communications, 1993. ICC '93 Geneva. Technical Program, Conference Record, IEEE International Conference on*, volume 2, pages 1064–1070 vol.2, May 1993.
- [17] Claude Berrou and Alain Glavieux. Near optimum error correcting coding and decoding: Turbo-codes. *Communications, IEEE Transactions on*, 44(10):1261–1271, 1996.
- [18] Peter Jung. Comparison of turbo-code decoders applied to short frame transmission systems. *Selected Areas in Communications, IEEE Journal on*, 14(3):530–537, 1996.
- [19] Ramesh Mahendra Pyndiah. Near-optimum decoding of product codes: block turbo codes. *Communications, IEEE Transactions on*, 46(8):1003–1010, 1998.
- [20] 3GPP. Ts 36.201 v8.3.0: LTE physical layer - general description (release 8), March 2009.
- [21] 3GPP. Ts 36.201 v10.0.0: LTE physical layer - general description (release 10), December 2010.

- [22] Jeanette Wannstrom for 3GPP. Lte-Advanced. <http://www.3gpp.org/technologies/keywords-acronyms/97-lte-advanced/>, June 2013.
- [23] A.S. Barbulescu and S.S. Pietrobon. Interleaver design for turbo codes. *Electronics Letters*, 30(25):2107–2108, Dec 1994.
- [24] H.R. Sadjadpour, N.J.A. Sloane, M. Salehi, and G. Nebe. Interleaver design for turbo codes. *Selected Areas in Communications, IEEE Journal on*, 19(5):831–837, May 2001.
- [25] Omer F Acikel and William E Ryan. Punctured turbo-codes for BPSK/QPSK channels. *Communications, IEEE Transactions on*, 47(9):1315–1323, 1999.
- [26] Robert G Gallager. Low-density parity-check codes. *Information Theory, IRE Transactions on*, 8(1):21–28, 1962.
- [27] Thomas J Richardson, Mohammad Amin Shokrollahi, and Rüdiger L Urbanke. Design of capacity-approaching irregular low-density parity-check codes. *Information Theory, IEEE Transactions on*, 47(2):619–637, 2001.
- [28] Sarah J Johnson. Introducing low-density parity-check codes.
- [29] Marc PC Fossorier, Miodrag Mihaljevic, and Hideki Imai. Reduced complexity iterative decoding of low-density parity check codes based on belief propagation. *Communications, IEEE Transactions on*, 47(5):673–680, 1999.
- [30] Tuomas Tirronen. *Optimizing the degree distribution of LT codes*. PhD thesis, Citeseer, 2006.

- [31] Iqbal Hussain, Ming Xiao, and Lars K Rasmussen. Error floor analysis of LT codes over the additive white gaussian noise channel. In *Global Telecommunications Conference (GLOBECOM 2011), 2011 IEEE*, pages 1–5. IEEE, 2011.
- [32] E. Hyytia, T. Tirronen, and J. Virtamo. Optimal degree distribution for LT codes with small message length. In *INFOCOM 2007. 26th IEEE International Conference on Computer Communications. IEEE*, pages 2576–2580, May 2007.
- [33] Qingxiao Du, Xiaoqin Song, Ying Liu, and Liping Zhao. Implementation of LT Code with a Novel Degree Distribution. *Open Journal of Applied Sciences*, 2(04):203, 2013.
- [34] Xianfeng ZENG, Fei GAO, and Xiangyuan BU. Performance of improved short-length raptor coded frequency-hop communication in partial-band interference.
- [35] Hrvoje Jenkac, Timo Mayer, Thomas Stockhammer, and Wen Xu. Soft decoding of LT-codes for wireless broadcast. *Proc. IST Mobile Summit 2005*, 2005.
- [36] Thomas Cover. Broadcast channels. *Information Theory, IEEE Transactions on*, 18(1):2–14, 1972.

- [37] Pulin Patel and Jack Holtzman. Analysis of a simple successive interference cancellation scheme in a DS/CDMA system. *Selected Areas in Communications, IEEE Journal on*, 12(5):796–807, 1994.
- [38] Weiwei Wang, Yanling Lu, Haibo Xu, and Hua Zhou. In-device coexistence interference evaluation and detection in LTE-A system. In *Vehicular Technology Conference (VTC Spring), 2012 IEEE 75th*, pages 1–5. IEEE, 2012.
- [39] Eduard Garcia Villegas, Elena Lopez-Aguilera, Rafael Vidal, and Josep Paradells. Effect of adjacent-channel interference in IEEE 802.11 WLANs. In *Cognitive Radio Oriented Wireless Networks and Communications, 2007. CrownCom 2007. 2nd International Conference on*, pages 118–125. IEEE, 2007.
- [40] Punit Rathod, Abhay Karandikar, and Anirudha Sahoo. Facilitating non-collocated coexistence for WiFi and 4G wireless networks. In *LCN*, pages 1–9, 2012.
- [41] John G Proakis. *Digital communications*. McGraw-Hill, New York, 1995.
- [42] 3GPP. Ts 26.346 v12.4.0: Multimedia broadcast/multicast service (MBMS); protocols and codecs (release 12), December 2014.
- [43] ETSI. Ts 102 472 v1.2.1: IP datacast over DVB-H: Content delivery protocols, December 2006.
- [44] T. Kasami and Shu Lin. Coding for a multiple-access channel. *Information Theory, IEEE Transactions on*, 22(2):129–137, Mar 1976.

- [45] Mohammad Jabbari Hagh and M Reza Soleymani. Raptor coding for non-orthogonal multiple access channels. In *Communications (ICC), 2011 IEEE International Conference on*, pages 1–6. IEEE, 2011.
- [46] Mohammad Jabbari Hagh and Mohammad Reza Soleymani. Application of raptor coding with power adaptation to DVB multiple access channels. *Broadcasting, IEEE Transactions on*, 58(3):379–389, 2012.
- [47] Simon Haykin. Cognitive radio: brain-empowered wireless communications. *Selected Areas in Communications, IEEE Journal on*, 23(2):201–220, 2005.
- [48] Qing Zhao and Brian M Sadler. A survey of dynamic spectrum access. *Signal Processing Magazine, IEEE*, 24(3):79–89, 2007.
- [49] Qualcomm and Ericsson. Introducing LTE in Unlicensed Spectrum. In *3GPP TSG RAN Meeting 62*, Busan, Korea, Dec. 3-6 2013.
- [50] Samsung. Samsung GALAXY S5. <http://www.samsung.com/global/microsite/galaxys5/features.html/>, April 2014.
- [51] Cisco. On LTE in Unlicensed Spectrum. In *3GPP TSG RAN Meeting 62*, Busan, Korea, Dec. 3-6 2013.
- [52] AT&T. Drivers, Benefits and Challenges for LTE in Unlicensed Spectrum. In *3GPP TSG RAN Meeting 62*, Busan, Korea, Dec. 3-6 2013.
- [53] Verizon. New band for LTE deployment as supplemental downlink in Unlicensed Spectrum 5.8 GHz in USA. In *3GPP TSG RAN Meeting 62*, Busan, Korea, Dec. 3-6 2013.

- [54] Nokia Corporation. LTE in unlicensed spectrum: European regulation and co-existence considerations. In *3GPP workshop on LTE-U*, Sophia Antipolis, France, Jun. 13 2014.
- [55] Cisco. Co-existence considerations for LTE-U. In *3GPP workshop on LTE-U*, Sophia Antipolis, France, Jun. 13 2014.
- [56] T-Mobile USA. T-MOBILE USA view on LTE carrier aggregation with unlicensed spectrum. In *3GPP workshop on LTE-U*, Sophia Antipolis, France, Jun. 13 2014.
- [57] Qualcomm. Extending the benefits of LTE to unlicensed spectrum. In *3GPP workshop on LTE-U*, Sophia Antipolis, France, Jun. 13 2014.
- [58] T. Nihtila, V. Tykhomyrov, O. Alanen, M.A. Uusitalo, A. Sorri, M. Moisio, S. Iraj, R. Ratasuk, and N. Mangalvedhe. System performance of lte and ieee 802.11 coexisting on a shared frequency band. In *Wireless Communications and Networking Conference (WCNC), 2013 IEEE*, pages 1038–1043, April 2013.
- [59] A.M. Cavalcante, E. Almeida, R.D. Vieira, F. Chaves, R.C.D. Paiva, F. Abinader, S. Choudhury, E. Tuomaala, and K. Doppler. Performance evaluation of lte and wi-fi coexistence in unlicensed bands. In *Vehicular Technology Conference (VTC Spring), 2013 IEEE 77th*, pages 1–6, June 2013.
- [60] Intel. LTE system deployment and performance in unlicensed bands. In *Tech Talk at IEEE ComSocEvent on LTE-U*, Nov. 12 2014.

- [61] JOEY JACKSON. CES 2015: Qualcomm takes on Wi-Fi with LTE-U. <http://www.rcrwireless.com/20150106/network-infrastructure/ces-2015-qualcomm-demonstrates-lte-u-tag20>, January 2015.
- [62] Zedomax. Download Booster on Galaxy S5 demo and howto! <https://www.youtube.com/watch?v=ub81ThPok2k>, April 2014.
- [63] Geek.com. Samsung gs5: How to enable and use download booster. <https://www.youtube.com/watch?v=0Z1MWGVj3yM>, April 2014.
- [64] Xiaowei Jin, Andrew W Eckford, and Thomas E Fuja. Analysis of joint channel estimation and LDPC decoding on block fading channels. In *International Symposium on Information Theory and its Applications, ISITA2004, Parma, Italy, 2004*.
- [65] Matthew C Valenti and Brian D Woerner. Iterative channel estimation and decoding of pilot symbol assisted turbo codes over flat-fading channels. *Selected Areas in Communications, IEEE Journal on*, 19(9):1697–1705, 2001.
- [66] Saikat Majumder and Shrish Verma. Joint channel estimation and decoding of Raptor code on fading channel. *Indian Journal of Computer Science and Engineering*, 4(2):168–173, 2013.